Bioorganic & Medicinal Chemistry 28 (2020) 115725

Contents lists available at ScienceDirect

Bioorganic & Medicinal Chemistry

journal homepage: www.elsevier.com/locate/bmc

Tetrahydroquinolinyl phosphinamidates and phosphonamidates enhancing tolerance towards drought stress in crops via interaction with ABA receptor proteins

Jens Frackenpohl[a,*], Luka J.B. Decker[a], Jan Dittgen[a], Jörg Freigang[c], Pierre Génix[b], Hendrik Helmke[a], Gudrun Lange[a], Peter Luemmen[a], Jana Schmidt[a], Dirk Schmutzler[a], Jean-Pierre Vors[b]

[a] Research & Development, Weed Control - Bayer AG, CropScience Division, Industriepark Höchst, D-65926 Frankfurt am Main
[b] Research & Development, Disease Control - Bayer S.A.S., Crop Science Division, CRLD, 14 Impasse Pierre Baizet, 69263 Lyon, France
[c] Research & Development, Research Technology, Bayer AG, CropScience Division, Gebäude 6240, Alfred-Nobel-Straße 50, 40789 Monheim, Germany

ARTICLE INFO

Keywords:
Phytochemistry
Drought stress
Phosphinamidates
Phosphonamidates
Abscisic acid receptor proteins

ABSTRACT

New phosphorous-containing lead structures against drought stress in crops interacting with RCAR/(PYR/PYL) receptor proteins were identified starting from in-depth SAR studies of related sulfonamide lead structures and protein docking studies. A converging 6-step synthesis via phosphinic chlorides and phosphono chloridates as key intermediates afforded envisaged tetrahydroquinolinyl phosphinamidates and phosphonamidates. Whilst tetrahydroquinolinyl phosphonamidates **13a,b** exhibited low to moderate target affinities, the corresponding tetrahydroquinolinyl phosphinamidates **12a,b** revealed confirmed strong affinities for RCAR/ (PYR/PYL) receptor proteins in Arabidopsis thaliana on the same level as essential plant hormone abscisic acid (ABA) combined with promising efficacy against drought stress *in vivo* (broad-acre crops wheat and canola).

1. Introduction

Agricultural crops face losses due to biotic stress such as pests, diseases, and weed damages, but abiotic stress adversely affects crop production even further in various parts of the world, decreasing average yields for most of the crops significantly.[1] Its impact is expected to grow as a consequence of climate change. Among various abiotic stress types affecting agricultural production, drought stress is considered to be the main source of crop losses around the globe.[2] So far, there are three major strategies for reducing the impact that drought has on crop yield. These include firstly exploiting beneficial effects of crop protection agents,[3] secondly developing drought tolerant crops through transgenic approaches or breeding,[4,5] but also exploring novel chemical active ingredients inspired by naturally occurring plant hormones or signaling pathways. Abscisic acid (**1**, *S*-(+)-ABA), a chiral sesquiterpenoid first discovered in the 1960 s,[6–9] is one of the most important plant hormones regulating developmental signals in plants such as seed maturation or dormancy. It also mediates the adaptation of plants to environmental abiotic stress types such as drought, heat or salinity stress by regulating transpiration. Interestingly, the application of ABA to wheat grown under near-field conditions improved water use efficiency without detectable growth trade-offs.[10] Thus, new synthetic small molecules that tune transpiration *via* the same mechanism as phytohormone ABA in anticipation of drought may be valuable tools for maximizing water use efficiency of crops thereby safeguarding crop yield. Studies on ABA mediated signaling have progressed rapidly since the discovery of RCAR/(PYR/PYL) receptor proteins as soluble ABA-receptors.[11,12] It was shown *via* crystal structural analysis that binding of ABA to RCAR12 induced a conformational change in the highly conserved ABA receptor proteins initiating an interaction with phosphoprotein phosphatases 2C (PP2Cs) thereby inhibiting their activity. Hence, these findings have granted new insights into the structure activity relationship (SAR) of ABA giving rise to novel synthetic analogues.

Whilst modifying the cyclohexenone moiety of ABA via stabilization or further substitution has attracted significant synthetic interest,[13–20] surprisingly few approaches have been made to identify open-chain analogues of ABA with promising target affinity. Recently, we have shown that cyano-cyclopropyl groups in **2a-c** served as suitable replacements of the cyclohexanone moiety leading to ABA analogues with

* Corresponding author.
E-mail address: jens.frackenpohl@bayer.com (J. Frackenpohl).

https://doi.org/10.1016/j.bmc.2020.115725
Received 10 July 2020; Accepted 18 August 2020
Available online 30 August 2020

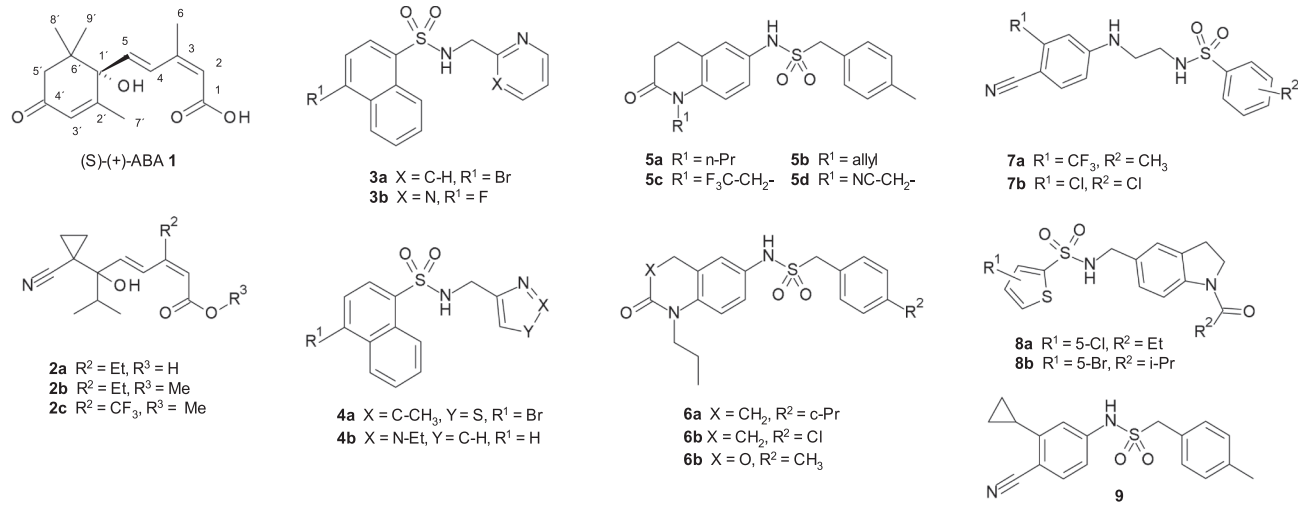

Figure 1. Abscisic acid, selected terpene analogues and sulfonamides interacting with RCAR/(PYR/PYL) receptor proteins.

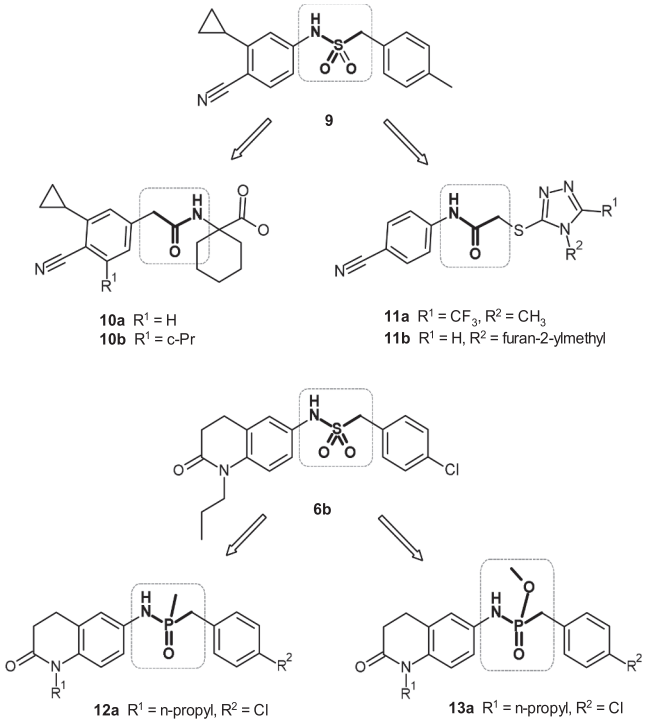

Figure 2. Synthetic non-sulfonamide ABA-receptor agonists, e.g. phenyl acetic acid amides, triazolyl thioacetamides, and target structures of the work described herein, i.e. phosphinamidates and phosphinamidates.

strong activity *in vitro* and *in vivo*.[21] Synthetic compounds interacting with RCAR/(PYR/PYL) receptor proteins have also been prepared by other groups.[22–24] Likewise, substituted aryl sulfonamides, e. g. 1st generation lead structure pyrabactin **3a**,[25,26] closely related pyrimidine **3b**, as well as thiazoles and pyrazoles **4a-b**,[27] have all shown promising initial receptor affinity and beneficial effects in *in vivo* tests (Fig. 1). Furthermore, tetrahydroquinolinyl sulfonamides, e.g. 2nd generation lead structure quinabactin **5a** and its close analogues **5b-d** with different *N*-substituents, with optimized phenyl substituents (**6a**) or ring modifications (**6b**) have shown even improved *in vitro* activity.[28–33] In our view this indicates that ABA analogues with more profound structural changes can be identified. More recently, 3rd generation sulfonamide lead structures that exhibit good receptor binding and promising *in vivo* efficacy in wheat have been identified *via* target-based high throughput screening (HTS), e.g. phenylsulfonyl ethylenediamines **7a-b**, and acylated indolinylmethyl sulfonamides **8a-b**.[34] It has been shown that *p*-cyano aniline moieties are effective isosteres of the carbonyl group in ABA's cyclohexenone headgroup. The beneficial impact of *p*-cyano aniline moieties on the interaction of agonists with ABA receptor proteins has also been observed in a structural analysis of the binding mode of sulfonamide-based 3rd generation agonist cyanabactin **9** with PYR1.[35] In good correlation with X-ray analyses of cyano cyclopropyl analogues of ABA (cf. **2a-c**),[23] this study showed that the 3-cyclopropyl-4-cyanoaniline moiety mimics the oxygen of ABA's cyclohexenone engaging the key components required to stabilize the activated receptors. However, the structural diversity of lead structures **3–9** is rather limited as they all share a central sulfonamide group. Herein, we outline how we identified new lead structures interacting with RCAR/(PYR/PYL) receptor proteins in which the sulfonamide moiety was replaced by phosphinamidates and phosphonamidates thus emphasizing opportunities to introduce further structural motifs into ABA-related structures.

2. Results and discussion

2.1. Structure-based design and modeling studies

From a synthetic chemist's perspective, various motifs could serve as replacements for the sulfonamide moiety linking substituted aryl or hetaryl groups in lead structures **3a, 5a, 8a,** and cyanabactin **9**, e.g. carboxamides, substituted ketones or phosphonamidates. Carboxamide spacers have already been investigated affording the first examples of non-sulfonamide ABA receptor agonists: Cyano- and cyclopropyl-substituted phenyl acetic acid amides **10a-b** and substituted triazolyl thioacetamides **11a-b** (with inverted acetamide units) have shown strong receptor binding (Fig. 2).[36,37] Interestingly, these promising hit structures share *p*-cyano-substituted phenyl groups with an additional group in the *meta*-position. This particular motif proved to be beneficial for strong receptor affinity in sulfonamides **7a-b** and **9**. To complement these approaches we have laid emphasis in our work outlined herein on further sulfonamide replacements. Based on our experience in agrochemical research we have chosen phosphorous-containing groups, i.e. phosphinamidates and phosphonamidates (cf. **12a, 13a**, Fig. 2).

Phosphoryl and carbonyl groups can act as a hydrogen-bond acceptor, whilst modifying strongly the physicochemical properties.[38] However, the number of bioactive molecules containing phosphinamidate or phosphonamidate motifs is rather limited compared to related sulfonamides.[39–42] Some famous examples are naturally occurring bialaphos and the potent herbicides phosphinotricine and glyphosate showing the biological potential of these motifs.

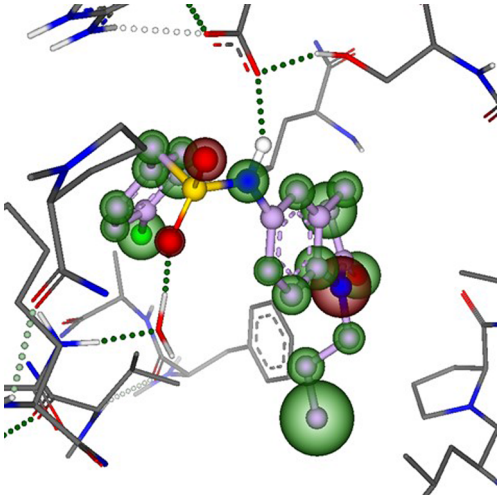

Figure 3. Interaction of **6b** with AtRCAR11 and the related phosphatase AtHAB1 as determined in the crystal structure. The H-bonds to glutamate 94 and to the water are indicated in dotted green lines. The contribution of individual atoms is indicated by spheres.[43] Green spheres show that these atoms stabilize the interaction, while red spheres indicate that these atoms destabilize the interaction. The size of the spheres correlates with the size of the contribution of the corresponding atoms.

In order to understand the impact of replacing the sulfur by a phosphorous atom, we analyzed the crystal structure of the complex between sulfonamide **6b** (with a Cl-atom instead of a methyl group in quinabactin **5a**) and *At*RCAR11 and the related phosphatase *At*HAB1 (Figure 3).

The crystal structure shows that the sulfonamide forms two essential hydrogen bonds to the ABA receptor. The sulfonamide amine interacts directly with the side chain of the conserved glutamate 94, whilst only one of the sulfonyl oxygens interacts with the backbone carbonyl group of histidine 60 *via* a bridging water molecule. The overall affinity is driven by a strong hydrophobic effect with a considerable contribution of the *N*-propyl moiety and the chlorine atom in the 4-position of the benzyl group.[34,35] Based on recognizing that only one sulfonyl oxygen is essential for receptor binding we selected prototypes of the envisioned *P*-isosteres of sulfonamides, e.g. phosphinamidate **12a** and phosphonamidates **13a & 13 m** (cf. Fig. 2, table 1), were docked into the ABA binding site of the crystal structure of ABA-bound *At*RCAR11 with related phosphatase *At*HAB1. Resulting poses were then scored using the HYDE scoring function (Fig. 3).[43]

Analyzing the binding mode of the *P*-methyl group in phosphinamidate **12a** *via* docking studies (Fig. 4a) indicated that there should be a very similar binding behaviour compared to sulfonamide **6b** in the X-ray structure (cf. Fig. 3). In particular, the H-bonds formed by the sulfonamide moiety are very well mimicked by the phosphinamidate group, and its methyl group fits nicely into a small hydrophobic pocket.

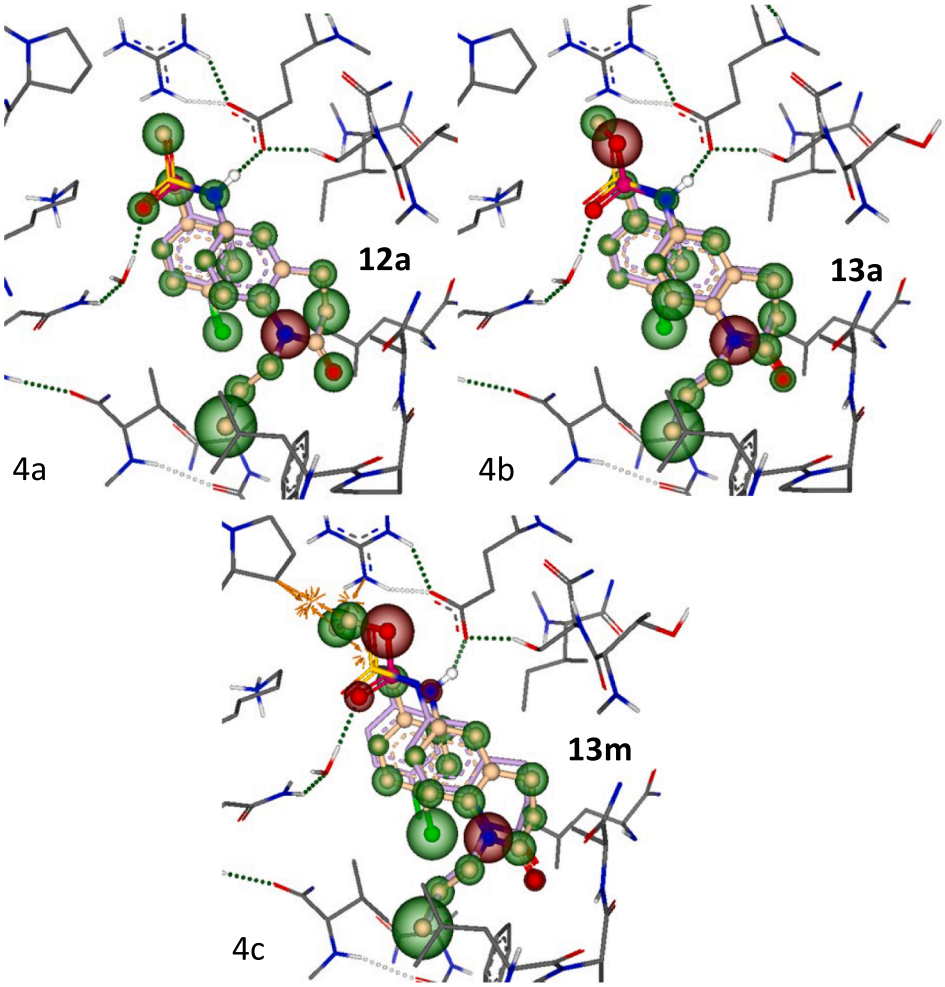

Figure 4. Modelled interaction of **12a** (a), **13a** (b) and **13 m** (c) with AtRCAR11 and the related phosphatase AtHAB1. The contribution of individual atoms is indicated by spheres.[43] Green spheres show that these atoms stabilize the interaction, while red spheres indicate that these atoms destabilize the interaction. The size of the spheres correlates with the size of the contribution of the corresponding atoms. Clashes in (c) are indicated by orange arrows. The crystal structure of **6b** is shown in mauve.

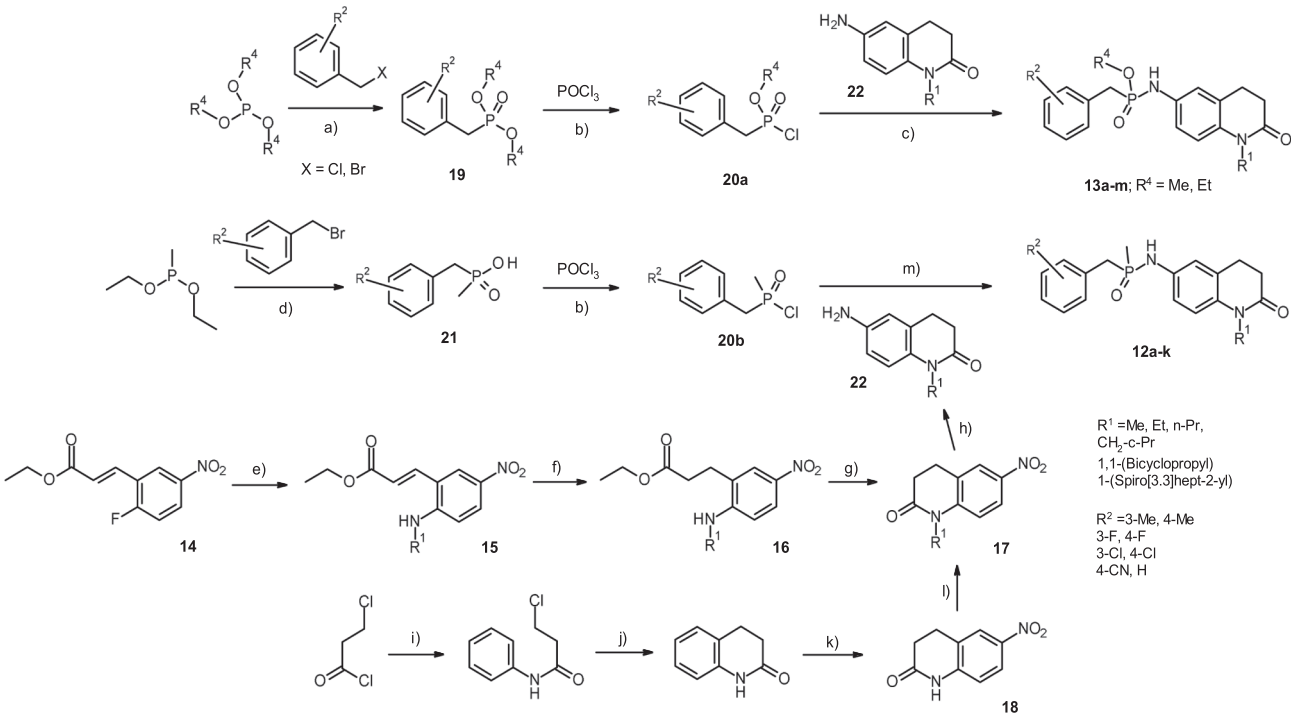

Scheme 1. Synthesis of tetrahydroquinolinyl phosphinamidates **12** and tetrahydroquinolinyl phosphonamidates **13**; (a) Trimethyl or triethyl phosphite, benzyl bromide, 100 °C, 10 h; (b) $POCl_3$, 60 °C, 1.5 h; (c) Et_3N, abs·THF, −20 °C – r.t, 1 h; (d) 1. *N,N*-DMF, 110 °C, 4 h, 2. aq. NaOH (10%), reflux, 2 h; (e) R^1-NH_2, *N,N*-DMF, $EtN(i\text{-}Pr)_2$, 50 °C, 16 h; (f) $(Ph_3P)_3RhCl$, abs. EtOH, H_2, r.t., 9 h; g) NaH, abs·THF, 0° C – r.t; h) $SnCl_2$-H_2O, abs. EtOH, 80 °C, 5 h; alternatively: Fe (powdered), NH_4Cl, $EtOH/H_2O$ (1:1); (i) Et_3N, substituted aniline, abs·THF, r.t., 2–6 h; (j) Friedel-Crafts alkylation with $AlCl_3$; (k) conc. H_2SO_4, conc. HNO_3, −20 °C – r.t., 4 h; (l) K_2CO_3, R^1-I, *N,N*-DMF, r.t., 24 h; (m) 1. $POCl_3$, 60 °C, 1.5 h, 2. Et_3N, abs·THF, −20 °C – r.t, 1 h.

The hydrophobic effect of small substituents in the *para*-position of the benzyl moiety (i.e. F, Cl, Me) contributed within our docking studies by roughly one pI_{50} unit to the overall binding affinity, while a benzyl moiety carrying a *p*-cyano group decreased the affinity due to the dehydration penalty that has to be paid for a polar group located in a hydrophobic pocket. These docking studies are in line with our experimental observations (cf. table 1). Substituents in the *meta*-position induced some movements of the benzylic moiety in order to avoid steric clashes which seem to weaken the binding. In addition, the *N*-Pr group contributed by two orders of magnitude to the pI_{50} values, while the smaller *N*-Me group stabilizes the binding only by one order of magnitude. As a consequence, combining a *N*-Me group at R^1 with a less favourably substituted benzyl moiety resulted in a loss of receptor affinity. These findings are in line with the observed *in vitro* and *in vivo* results outlined in table 1. When replacing the phosphinamidate's methyl group by a methoxy group, thus affording the related phosphonamidate, there seemed to be still enough space, and no significant movement of the respective phosphonamidate was required in the docking study to avoid steric clashes (Figure 4b). The slightly lower affinity may be due to the polar dehydration of the bridging oxygen, but the same SAR applies. Larger hydrophobic substituents at position R^1 such as *N*-CH_2-c-Pr, *N*-1,1'-(bicyclopropyl) or *N*-1-(spiro[3.3]hept-2-yl) seemed to have similar hydrophobic effects as the *N*-propyl moiety. However, increasing the phosphonamidate substituent at the *P*-centred position R^3 by introducing an ethoxy group (**13 m**, Figure 4c) showed in our docking study that steric clashes with the amino acids proline 55, arginine 79 and glutamate 94 require a significant movement of **13m** in order to fit into the binding pocket. Likewise, these phosphonamidates (R^3 = OEt) could not assume a pose without significant steric clashes, while maintaining the H-bonds. This may explain why phosphonamidates **13k-13o** neither showed binding to the ABA receptor nor *in vivo* effects.

2.2. Chemistry

Based on our experiences with the synthesis of tetrahydroquinolinyl sulfonamides[30,31] two main synthetic approaches were used to prepare tetrahydroquinolinyl amines. Firstly, dihydroquinolin-2(1*H*)-one which was accessible *via* Friedel-Crafts acylation could be easily converted into the corresponding intermediate **22** via direct nitration, *N*-alkylation with a primary sterically less demanding alkyl halide and Fe- or $SnCl_2$-mediated reduction of the nitro group. Secondly, the desired *N*-substituted 6-amino 3,4-dihydroquinolin-2(1*H*)-ones **22** were prepared in 4 steps *via* (i) S_NAr reaction of 6- ethyl (2*E*)-3-(2-fluoro-5-nitrophenyl)acrylate **14** with a suitable amine, preferably an amine with a larger substituent, (ii) hydrogenation of the acrylic double bond with Wilkinson's catalyst, (iii) lactam formation and (iv) subsequent reduction of the nitro group. The second approach proved to be particularly suitable for sterically demanding amines or cycloalkyl amines, whilst the first approach worked well with sterically less demanding alkyl halides (e.g. *n*-propyl iodide or chloromethylcyclopropane). Likewise, 1,1′-bi(cyclopropyl)-1-amine reacted easily with fluorinated phenyl acrylate **14** to afford intermediate **15** giving access to desired phosphonamides **13 h** and **13n**.

Substituted phosphinic chlorides and phosphono chloridate precursors could be prepared, for example, in a stepwise approach starting with the reaction of a correspondingly substituted benzyl halide and a substituted phosphorus compound such as trimethylphosphite, triethyl phosphite, or diethylmethyl phosphonite using *Arbuzov* conditions in a suitable polar-aprotic solvent (e.g. *N,N*-dimethylformamide or Et_2O). Alternatively, using a suitable base (e.g. sodium hydroxide) at elevated temperature, diethyl methylphosphonite could be converted into the corresponding acid intermediate **21** (cf. Scheme 1). In the next step, the intermediates **19** and **21** obtained in this manner could be converted into the corresponding phosphinic chloride and phosphono chloridate

Table 1

SAR-results of tetrahydroquinolinyl phosphinamidates **12** and phosphonamidates **13.**

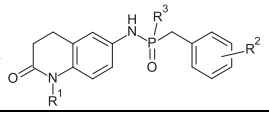

Entry	No.	Substituents[a]			*In vitro* activity - ABI1(AtRCAR)[b]		*In vivo* efficacy vs. drought stress [250 g/ha][c]	
		R^1	R^2	R^3	Activity [%] 5 μM	pI_{50}	Wheat[c]	Canola[c]
1	**12a**	n-Pr	4-Cl	Me	+ + +	4.6	+ +	+ +
2	**12b**	n-Pr	4-Me	Me	+ + + +	5.7	+ +	+ + +
3	**12c**	n-Pr	4-F	Me	+ + + +	4.9	+ +	+ + +
4	**12d**	n-Pr	3-Me	Me	+ + +	4.3	+	+ +
5	**12e**	n-Pr	3-F	Me	+ + +	4.3	+ + +	+ +
6	**12f**	Me	4-Me	Me	+ + +	4.3	+	+ +
7	**12g**	Me	4-Cl	Me	+ +	4.3	+	+ +
8	**12h**	Me	3-F	Me	-	n.d.	0	0
9	**12i**	Me	3-Cl	Me	-	n.d.	0	0
10	**12j**	Me	4-CN	Me	+	n.d.	0	+
11	**12k**	n-Pr	H	Me	-	n.d.	0	0
12	**13a**	n-Pr	4-Cl	OMe	+ + +	4.4	+ +	+ +
13	**13b**	n-Pr	4-Me	OMe	+ +	4.0	+	+ +
14	**13c**	n-Pr	4-F	OMe	+ +	4.0	+	+
15	**13d**	n-Pr	4-CN	OMe	+	n.d.	0	+
16	**13e**	Me	4-Me	OMe	-	n.d.	0	0
17	**13f**	Et	4-Me	OMe	+	n.d.	0	+
18	**13g**	CH_2-c-Pr	4-Me	OMe	+ +	4.2	+ +	+ +
19	**13h**	1,1'-(Bicyclopropyl)	4-Me	OMe	+ +	4.0	+ +	+
20	**13i**	1-(Spiro[3.3]hept-2-yl)	4-Me	OMe	+ +	4.0	+	+
21	**13j**	Me	4-Cl	OMe	-	n.d.	0	0
22	**13k**	n-Pr	3-F	OMe	-	n.d.	0	0
23	**13l**	n-Pr	4-Me	OEt	-	n.d.	0	0
24	**13m**	n-Pr	4-Cl	OEt	-	n.d.	0	0
25	**13n**	CH_2-c-Pr	4-Me	OEt	-	n.d.	0	0
26	**13o**	1,1'-(Bicyclopropyl)	4-Me	OEt	-	n.d.	0	0
27	**5a**	n-Pr	4-Me	Sulfonamide	+ + + +	5.9	+ +	+ +
28	**1**	Abscisic acid			+ + + +	7.0	+ + +	+ + +

[a] c-Pr = cyclopropyl, c-Bu = cyclobutyl, i-Pr = isopropyl; [b] a final expert assessment of target affinity was made according to the following classification: "-": < 30% , "+" = 30% < activity < 50%, "+ +" = 50% < activity < 70%, "+ + +" = 70% < activity < 90%, "+ + + +" = activity > 90%; [c] standard application rate for crop protection greenhouse trials; [d] a final expert assessment of efficacies was made according to the following classification: "0" = no effect, "+" = slight beneficial effect, "+ +" = significant beneficial effect, "+ + +" = strong beneficial effect against drought stress, "+ + + +" = very strong effect superior to internal standard ABA (comparative visual assessment of greenmass).

precursors (e.g. **20a,b**, Scheme 1).[44–46] Coupling of the substituted phosphonyl chloride (**20**) and phosphinyl chloride precursors with the appropriate oxotetra-hydroquinolinyl amines **22** with the aid of a suitable base (e.g. triethylamine, pyridine) under mild conditions in an aprotic solvent (e.g. tetrahydrofuran, acetonitrile, or dichloromethane) afforded the desired tetrahydroquinolinyl phosphinamidates and -phosphonamidates **13a-n** and **12a-k**.[47] The formation of *P—N* bonds remains a challenge as is shown by low to moderate yields in the final *P—N* coupling step of compounds **20** and **21** with amines **22** (Scheme 1). Furthermore, only a limited number of literature citations for the formation of phosphinamidates and related phosphonamidates can be found.[48] Following the synthetic approaches outlined in scheme 1 we have prepared target compounds covering structural variations at three positions, firstly at the tetrahydroquinolinyl nitrogen (N-R^1), secondly in the *P*-benzyl moiety (R^2) and finally at the central phosphorous atom (*P*-R^3).

2.3. SAR study

All compounds that have been prepared to explore the SAR of tetrahydroquinolinyl phosphinamidates **12** and phosphon-amidates **13** were tested both, for target affinity in dedicated *in vitro* tests, as well as for beneficial effects *in vivo* under drought stress conditions upon foliar application on plants. Wheat and Canola were chosen as model plants for monocotyledonous and dicotyledonous species, whereas *in vitro* tests were carried out using the ABA-receptor RCAR11 in *Arabidopsis thaliana*.

Strong receptor affinity could be observed for phosphinamidates carrying halogen or methyl substituents in the *P*-benzyl moiety combined with an *n*-Pr substituent at the tetrahydroquinolinyl nitrogen, albeit with lower pI_{50} values than ABA **1** as the internal standard (Table 1). *P*-benzyl moieties carrying substituents in the 4-position of the aryl unit afforded most promising binding affinities in line with results from earlier studies in the field of tetrahydroquinolinyl sulfonamides. In particular, phosphinamidates carrying an unbranched *n*-Pr substituent in the *N*-R^1 moiety together with a 4-Cl-benzyl group (**12a**, Table 1, entry 1), a 4-Me-benzyl group (**12b**, entry 2) and a 4-F-benzyl moiety (**12c**, entry 3) as the *P*-substituent showed very good target affinities together with promising efficacy against drought stress *in vivo*, preferably in canola. Whilst introducing a small methyl substituent at position R^1 in combination with a 4-substituted *P*-benzyl group afforded weaker effects, both *in vitro* and *in vivo* (**12f**, **12 g**, **12j**, cf. Table 1, entries 6, 7, 10), a shift from 4- to 3-substituted *P*-benzyl moieties was tolerated in *N*-(*n*-Pr)-tetrahydroquinolinyl phosphinamidates (**12d**, **12e**, Table 1, entries 4,5). Remarkably, 3-F-benzyl substituted phosphinamidate **12e** exhibited the strongest effects of all new compounds against drought stress *in vivo* in wheat. Remarkably, these effects are on the level of ABA **1** (Table 1, entry 28). Introducing two structural variations compared with the strongest *in vitro* hit **12b**, i.e. replacing the *n*-Pr group by Me and changing the *P*-benzyl substitution from the 4- to 3-position or to an unsubstituted phenyl group, led to a complete loss of activity, both *in vitro* and *in vivo* (**12 h, 12i, 12j, 12 k,** cf.

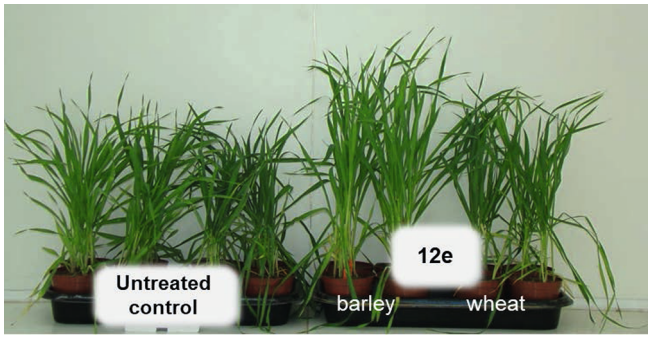

Figure 5. Advanced drought stress trials with **12e** in wheat and barley under moderate stress conditions, i.e. 45% damage for barley and 44% for wheat, respectively.

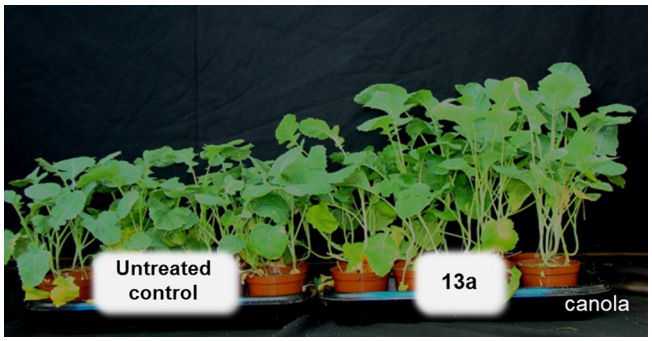

Figure 6. Advanced drought stress trials with **13a** in canola under moderate stress conditions, i.e. 48% damage.

Table 1, entries 8–11). Hence, phosphinamidates **12** proved to be highly sensitive towards changes in the substitution pattern. These observations are in line with the docking studies outlined above.

Likewise, phosphonamidates **13** also showed a high sensitivity towards structural changes. Whilst *N*-(*n*-Pr)-tetrahydroquinolinyl phosphonamidates bearing a *p*-substituted *P*-benzyl moiety and a *P*-OMe group (**13a-13c**, Table 1, entries 12–14) exhibited significant target affinities, related analogues with smaller *N*-substituents in the tetrahydroquinolinyl moiety showed weaker or no target affinity and proved to be inactive *in vivo* (cf. **13e**, **13f**, **13j**, Table 1, entries 16, 17, 21). Furthermore, phosphonamidates **13a-13c** afforded weaker activities, both *in vitro* and *in vivo*, than corresponding phosphinamidates **12a-12c**. We thus investigated the impact of *N*-substituents in the tetrahydroquinolinyl moiety of phosphonamidates further by carefully modifying the *n*-Pr group and keeping the other substituents constant (i.e. *p*-Me benzyl and OMe substituents on the phosphorous atom). Based on promising results obtained in earlier studies of *N*-substituted tetrahydroquinolinyl sulfonamides[30,31] larger substituents such as cyclopropyl-methyl (**13 g**), 1,1′-(bicyclopropyl) (**13 h**), and 1-(spiro[3.3] hept-2-yl) (**13i**) were synthesized affording moderate target affinities and moderate effects *in vivo* with **13 g** showing the best results. In contrast to a change from *N*-(*n*-Pr) to *N*-Me activity *in vitro* and *in vivo* was preserved upon introducing these particular *N*-substituents. However, they did not afford improved effects as shown in the related tetrahydroquinolinyl sulfonamides.[30,31] A change of the *P*-benzyl substituent from the *para*- to the *meta*-position led to a loss of activity, both *in vitro* and *in vivo* (**13 k**, Table 1, entry 22). Changing the alkoxy substituent (R^3) in the central phosphonamidate moiety from a methoxy to an ethoxy group caused a significant decline in target affinity in line with a loss of *in vivo* efficacy as is shown by results obtained for target compounds **13 l-13o** (Table 1, entries 23–26).

In addition to reference plant hormone ABA **1**, we have tested tetrahydroquinolinyl sulfonamide **5a**, one of the sulfonamide lead structures outlined in Fig. 1, in our *in vitro* and *in vivo* tests. Remarkably, closely related phosphinamidate **12b** (R^1 = *n*-Pr, R^2 = p-Me) showed a comparable target affinity combined with better efficacy against drought stress in canola. Phosphinamidate **12c** and **12e** also showed stronger efficacy *in vivo* than sulfonamide **5a**. Remarkably, phosphonamidate **13g** exhibited significant effects *in vivo* against drought stress, both in wheat and canola, although its target affinity was only moderate (pI_{50} 4.2). The phosphinamidate and phosphonamidate moieties in compounds **12** and **13** prepared in our SAR-study thus serve as a suitable bioisosteric replacement of the sulfonamide moiety in tetrahydroquinolinyl sulfonamides (e.g. **5a**, **6b**).

To further validate our initial *in vivo* screening results, we selected **12e** with strong efficacy in wheat and **13a** with good efficacy in canola as prototypes for advanced greenhouse trials (i.e. more replicates, different application rates, e.g. 100 and 25 g/ha, additional crops such as corn and barley, different corn varieties and moderate stress levels). Accordingly, significant beneficial effects against drought stress could be observed in wheat, and particularly in barley compared to untreated controls upon treatment with **12e** as the representative phosphinamidate (Fig. 5).

Interestingly, the promising *in vivo* efficacy of several phosphonamidates observed in our initial screening (cf. Table 1) could be confirmed as representative example **13a** afforded significant beneficial effects under moderate drought stress conditions in canola (Fig. 6).

3. Conclusions

We have identified new phosphorous-containing ABA-receptor agonists showing activity against drought stress in field crops by interacting with RCAR/(PYR/PYL) receptor proteins. These new substituted phosphinamidates and phosphonamidates were identified starting from SAR studies of related sulfonamide lead structures and protein docking studies. The docking studies showed that both phosphorous moieties could serve as bioisosteric replacements of the sulfonyl group in known sulfonamide ABA-receptor agonists. A converging 6-step synthesis proceeding *via* phosphinic chlorides and phosphono chloridates as key intermediates has been developed to afford envisaged tetrahydroquinolinyl phosphinamidates **12** and phosphonamidates **13**. Whilst phosphonamidates **13a-o** exhibited low to moderate target affinities, the corresponding phosphin-amidate **12b** revealed good affinities for RCAR/ (PYR/PYL) receptor proteins in *Arabidopsis thaliana* on the same level as structurally related sulfonamide-based lead structure quinabactin. Remarkably, **12b** showed promising efficacy against drought stress *in vivo* (broad-acre crops wheat and canola). Furthermore, tetrahydroquinolinyl phosphonamidates (e.g. **13a**) proved to be active against drought stress *in vivo*. Our results demonstrate that phosphinamidates **12** and phosphonamidates **13** are effective isosteres of the sulfonyl group in tetrahydroquinolinyl sulfonamide-based ABA-receptor agonists, thus nicely complementing earlier work in this field. These results should encourage other chemists involved in life science research to use phosphorous-based chemistry in their work.

4. Experimental

4.1. Biology

4.1.1. In vivo studies

Seeds of monocotyledonous and dicotyledonous crop plants were laid out in sandy loam in wood-fiber pots, covered with soil and cultivated in a greenhouse under good growth conditions. The test plants were treated at the first leaf stage (BBCH10 – BBCH13). To ensure uniform water supply before commencement of drought stress, the potted plants were supplied with the maximum amount of water immediately beforehand by dam irrigation and, after application, transferred into plastic inserts in order to prevent subsequent, excessively rapid drying. The respective compounds, formulated in the form of wettable powders (WP) or emulsion concentrates (EC), were sprayed

onto the green parts of the plants as an aqueous suspension at an equivalent water application rate of 600 l/ha with addition of 0.2% wetting agent (agrotin). Substance application is followed immediately by drought stress treatment of the plants. Drought stress was induced by gradual drying out under the following conditions: "day" = 14 h with illumination at 26 °C; "night" = 10 h without illumination at 18 °C. The duration of the respective stress phases was guided mainly by the state of the untreated (=treated with blank formulation but without test compound), stressed control plants and thus varied from wheat to canola. It was ended (by re-irrigating or transfer to a greenhouse with standard growth conditions) as soon as irreversible damage was observed on the untreated, stressed control plants. In the case of dicotyledonous crops, for example canola, the duration of the drought stress phase varied between 3 and 5 days; in the case of monocotyledonous crops, for example wheat, it varied between 6 and 10 days. The end of the stress phase was followed by an approx. 5–7-day recovery phase, during which the plants were once again kept under good growth conditions in a greenhouse. In order to rule out any influence of the effects observed by any fungicidal action of the test compounds, it was additionally ensured that the tests proceeded without fungal infection and without infection pressure. After the recovery phase had ended, the intensities of damage were rated visually in comparison to untreated, unstressed controls of the same age (in the case of drought stress). The intensity of damage was first recorded as a percentage (100% = plants have died, 0% = like control plants). These values were then used to calculate the efficacy of the test compounds (=percentage reduction in the intensity of damage as a result of substance application), and a final assessment of the respective efficacy was made, i.e. "0" = no effect, "+" = slight beneficial effect, "++" = significant beneficial effect, "+++" = strong beneficial effect against drought stress, "++++" = very strong beneficial effect superior to internal standard ABA.

4.1.2. In vitro - AtABI1-(AtRCAR11)

The assay described hereinafter utilizes the inhibition of the phosphatase *At*ABI1 *via* the co-regulator RCAR11/PYR1 from *Arabidopsis thaliana*. Expression and purification of RCARs and PP2Cs was performed as described.[11] A concise overview of the correlation between PYR/PYL and RCAR numbering can be found in reference by Grill et al.[49] For the determination of activity, the dephosphorylation of 4-methylumbelliferyl phosphate (MUP) was measured at 460 nm. The *in vitro* assay was conducted in Greiner 96-well, 384-well or 1536-well PS microplates, using two controls: a) dimethyl sulfoxide (DMSO) 0.5% (f.c.) and b) 5 µM (f.c.) abscisic acid (ABA). For high throughput screening 1 µg/ml ABI1 and 0,5 µg/ml RCAR11 were incubated with 100 µM MUP in reaction buffer (50 mM Tris/HCl pH 7.8, 50 mM NaCl, 0.3 mM MnCl2, 0.01% Tween, 0.01% BSA) at 32 °C for 80 min. Fluorescence intensity was detected by a BMG Labtech Pherastar using a 340 nm excitation filter and a 460 nm emission filter. For follow up compound characterization the assay was conducted with substance concentrations of the appropriate chemical test substances in a concentration range of 0.1 µM to 100 µM in a solution of DMSO and water. The substance solution thus obtained, if necessary, was stirred with esterase from porcine liver (EC 3.1.1.1) at room temperature for 3 h and centrifuged at 4000 rpm for 30 min. A total volume of 45 µl was introduced into each cavity of the microplate, having the following composition: 1. 5 µl of substance solution, i.e. a) DMSO 5% or b) abscisic acid solution or c) the corresponding example compound of the general formula (I) dissolved in 5% DMSO. 2. 20 µl of enzyme buffer mix, composed of a) 40% by vol. of enzyme buffer [10 ml contain equal proportions by volume of 500 mM Tris-HCl pH8, 500 mM NaCl, 3.33 mM $MnCl_2$, 40 mM dithiothreitol (DTT)], b) 4% by vol. of *At*ABI1 or *Ta*ABI1 dilution (protein stock solution was diluted so as to give, after addition, a final concentration in the assay of 0.15 µg ABI1/well), c) 4% by vol. of *At*RCAR11 dilution (enzyme stock was diluted so as to give, on addition of the dilution to the enzyme buffer mix, a final concentration in the assay of 0.30 µg enzyme/well), d) 5% by vol. of Tween20 (1%), e) 47% by vol·H_2O bi-dist. 3. 20 µl of substrate mix, composed of a) 10% by vol. of 500 mM Tris-HCl pH8, b) 10% by vol. of 500 mM NaCl, c) 10% by vol. of 3.33 mM $MnCl_2$, d) 5% by vol. of 25 mM MUP, 5% by vol. of Tween20 (1%), 60% by vol. of H_2O bi-dist. Enzyme buffer mix and substrate mix were freshly made 5 min prior to the addition and warmed to a temperature of 35 °C. On completion of pipetting of all the solutions and on completion of mixing, the plate was incubated at 35 °C for 20 min. Finally, a relative fluorescence measurement was made at 35 °C with a BMG Labtech "POLARstar Optima" microplate reader using a 340/10 nm excitation filter and a 460 nm emission filter. An expert assessment of target affinity was made according to the following classification: "-": < 30% , "+" = 30% < activity < 50%, "++" = 50% < activity < 70%, "+++" = 70% < activity < 90%, "++++" = activity > 90%.

4.2. Chemistry

4.2.1. General

All reagent-grade solvents and chemicals were purchased from standard commercial suppliers and used without further purification. All non-aqueous reactions were carried out under anhydrous conditions using dry solvents. Reactions were monitored by LC-MS or TLC carried out on 0.25 mm silica gel plates (60F-254). TLC plates were visualized using UV light. Flash chromatography was carried out using Biotage Isolera One systems with pre-packed column cartridges (Biotage KP-Sil [40 + M] or KP-Sil [25 + M]). The ^{1}H NMR, ^{13}C NMR and ^{19}F NMR spectroscopy data which are reported for the chemical examples described below (400 MHz for ^{1}H NMR and 150 MHz for ^{13}C NMR and 375 MHz for ^{19}F NMR, solvent: $CDCl_3$, CD_3OD or d_6-DMSO, internal standard: tetramethylsilane δ = 0.00 ppm), were obtained on a Bruker instrument, and the signals listed have the meanings given below: br = broad; s = singlet, d = doublet, t = triplet, dd = doublet of doublets, ddd = doublet of a doublet of doublets, m = multiplet, q = quartet, quint = quintet, sext = sextet, sept = septet, dq = doublet of quartets, dt = doublet of triplets. The abbreviations used for chemical groups or dedicated hydrogen atoms are defined as follows: Me = CH_3, Et = CH_2CH_3, *t*-Hex = $C(CH_3)_2CH(CH_3)_2$, *t*-Bu = $C(CH_3)_3$, *n*-Bu = unbranched butyl, *n*-Pr = unbranched propyl, *c*-Hex = cyclohexyl, *Ar*H = aromatic hydrogen, *Het*H = heteroaromatic hydrogen. In the case of diastereomeric mixtures, either the significant signals for each of the diastereomers or the characteristic signal of the main diastereomer is/are reported. In the following sections, the yield for the corresponding phosphinamidates ***12a-k*** and phosphonamidates **13a-o** is given as a combined yield over 3–4 steps as most of the phosphorous chemistry was carried out with purification of the final product only.

4.2.2. Preparation of phosphinamidates *12a-k*

All cpds were prepared following the protocol outlined for the synthesis of **12k**.

4.2.2.1. *P-(4-Chlorobenzyl)-P-methyl-N-(2-oxo-1-propyl-1,2,3,4-tetrahydroquinolin-6-yl)phosphinamidate (**12a**)*.

White solid; yield 11%; ^{1}H NMR (400 MHz, $CDCl_3$) δ 7.17–7.07 (m, 5H), 6.89 (m, 1H), 6.62 (m, 1H), 6.57 (br. s, 1H, NH), 3.86 (m, 2H), 3.35–3.23 (m, 2H), 2.83 (m, 2H), 2.62 (m, 2H), 1.68–1.59 (m, 2H), 1.52 (d, 3H), 0.95 (t, 3H). LCMS (ESI, *m/z*): $[M+H]^+$ 391.9. HRMS (ESI, *m/z*): calcd. for $C_{20}H_{24}N_2O_2PCl$, 390.8435 $[M+H]^+$; found 390.8418.

4.2.2.2. *P-(4-Methylbenzyl)-P-methyl-N-(2-oxo-1-propyl-1,2,3,4-tetrahydroquinolin-6-yl)phosphinamidate (**12b**)*.

White solid; yield 14%; ^{1}H NMR (400 MHz, $CDCl_3$ δ, ppm) 7.13 (m, 2H), 7.07 (m, 2H), 6.92 (m, 2H), 6.86 (m, 2H), 3.86 (m, 2H), 3.39–3.21 (m, 2H), 2.83 (m, 2H), 2.62 (m, 2H), 2.32 (s, 3H), 1.68–1.58 (m, 2H), 1.51 (d, 3H), 0.95 (t, 3H); LCMS (ESI, *m/z*): $[M]^+$ 370.4; HRMS (ESI, *m/z*): calcd. for $C_{21}H_{27}N_2O_2P$, 370.1810 $[M+H]^+$; found 370.1819.

*4.2.2.3. P-(4-Fluorobenzyl)-P-methyl-N-(2-oxo-1-propyl-1,2,3,4-tetrahydroquinolin-6-yl)phosphinamidate (**12c**)*. White solid; yield 19%; ^{1}H NMR (400 MHz, $CDCl_3$ δ, ppm) 7.15 (m, 2H), 7.02 (m, 2H), 6.92 (m, 2H), 6.87 (m, 2H), 4.54 (m, 1H), 3.86 (m, 2H), 3.35–3.23 (m, 2H), 2.84 (m, 2H), 2.62 (m, 2H), 1.68–1.59 (m, 2H), 1.52 (d, 3H), 0.95 (t, 3H); LCMS (ESI, *m/z*): $[M+H]^+$ 375.4; HRMS (ESI, *m/z*): calcd. for $C_{20}H_{24}N_2O_2PF$, 374.1559 $[M+H]^+$; found 374.1549.

*4.2.2.4. P-(3-Methylbenzyl)-P-methyl-N-(2-oxo-1-propyl-1,2,3,4-tetrahydroquinolin-6-yl)phosphinamidate (**12d**)*. White solid; yield 9%; ^{1}H NMR (400 MHz, $CDCl_3$ δ, ppm) 7.19 (m, 1H), 7.09–6.96 (m, 2H), 6.94–6.81 (m, 5H), 3.89 (m, 2H), 3.44–3.27 (m, 2H), 2.87 (m, 2H), 2.65 (m, 2H), 1.72–1.60 (m, 2H), 1.56 (d, 3H), 0.98 (t, 3H); LCMS (ESI, *m/z*): $[M]^+$ 370.4; HRMS (ESI, *m/z*): calcd. for $C_{21}H_{27}N_2O_2P$, 370.1810 $[M+H]^+$; found 370.1802.

*4.2.2.5. P-(3-Fluorobenzyl)-P-methyl-N-(2-oxo-1-propyl-1,2,3,4-tetrahydroquinolin-6-yl)phosphinamidate (**12e**)*. White solid; yield 8%; ^{1}H NMR (400 MHz, $CDCl_3$ δ, ppm) 7.33 (m, 1H), 7.01–6.95 (m, 2H), 6.93–6.88 (m, 3H), 6.87 (m, 2H), 3.89 (m, 2H), 3.44–3.27 (m, 2H), 2.87 (m, 2H), 2.65 (m, 2H), 1.72–1.60 (m, 2H), 1.56 (d, 3H), 0.98 (t, 3H); LCMS (ESI, *m/z*): $[M+H]^+$ 375.4; HRMS (ESI, *m/z*): calcd. for $C_{20}H_{24}N_2O_2PF$, 374.1559 $[M+H]^+$; found 374.1545.

*4.2.2.6. P-(4-Methylbenzyl)-P-methyl-N-(2-oxo-1-methyl-1,2,3,4-tetrahydroquinolin-6-yl)phosphinamidate (**12f**)*. White solid; yield 17%; ^{1}H NMR (400 MHz, $CDCl_3$ δ, ppm) 7.13 (m, 2H), 7.09–7.03 (m, 3H), 6.98 (m, 1H), 6.79 (m, 1H), 6.58–6.52 (m, 1H), 3.39–3.23 (m, 2H), 3.29 (s, 3H), 2.86–2.77 (m, 2H), 2.63–2.57 (m, 2H), 1.52 (d, 3H); LCMS (ESI, *m/z*): $[M+H]^+$ 353.3.

*4.2.2.7. P-(4-Chlorbenzyl)-P-methyl-N-(2-oxo-1-methyl-1,2,3,4-tetrahydroquinolin-6-yl)phosphinamidate (**12 g**)*. White solid; yield 8%; ^{1}H NMR (400 MHz, $CDCl_3$ δ, ppm) 7.28 (m, 2H), 7.12 (m, 2H), 6.92 (m, 2H), 6.86 (m, 1H), 4.54 (m, 1H), 3.35–3.26 (m, 2H), 3.32 (s, 3H), 2.86 (m, 2H), 2.64 (m, 2H), 1.52 (d, 3H); LCMS (ESI, *m/z*): $[M+H]^+$ 363.8.

*4.2.2.8. P-(3-Fluorbenzyl)-P-methyl-N-(2-oxo-1-methyl-1,2,3,4-tetrahydroquinolin-6-yl)phosphinamidate (**12 h**)*. White solid; yield 12%; ^{1}H NMR (400 MHz, $CDCl_3$ δ, ppm) 7.28 (m, 1H), 6.99–6.93 (m, 4H), 6.90–6.82 (m, 2H), 4.54 (m, 1H), 3.42–3.24 (m, 2H), 3.32 (s, 3H), 2.86 (m, 2H), 2.63 (m, 2H), 1.53 (d, 3H); LCMS (ESI, *m/z*): $[M+H]^+$ 347.3.

*4.2.2.9. P-(3-Chlorbenzyl)-P-methyl-N-(2-oxo-1-methyl-1,2,3,4-tetrahydroquinolin-6-yl)phosphinamidate (**12i**)*. White solid; yield 11%; ^{1}H NMR (400 MHz, $CDCl_3$ δ, ppm) 7.33 (m, 1H), 7.18–7.06 (m, 4H), 6.92 (m, 2H), 6.86 (m, 1H), 4.54 (m, 1H), 3.35–3.26 (m, 2H), 3.32 (s, 3H), 2.86 (m, 2H), 2.64 (m, 2H), 1.52 (d, 3H); LCMS (ESI, *m/z*): $[M]^+$ 362.8. HRMS (ESI, *m/z*): calcd. for $C_{18}H_{20}N_2O_2PCl$, 362.0951 $[M+H]^+$; found 362.0966.

*4.2.2.10. P-(4-Cyanobenzyl)-P-methyl-N-(2-oxo-1-methyl-1,2,3,4-tetrahydroquinolin-6-yl)phosphinamidate (**12j**)*. White solid; yield 14%; ^{1}H NMR (400 MHz, $CDCl_3$ δ, ppm) 7.61 (m, 2H), 7.32 (m, 2H), 6.94 (m, 2H), 6.85 (m, 1H), 4.56 (m, 1H), 3.42–3.25 (m, 2H), 3.32 (s, 3H), 2.87 (m, 2H), 2.64 (m, 2H), 1.52 (d, 3H); LCMS (ESI, *m/z*): $[M+H]^+$ 354.3.

*4.2.2.11. P-Benzyl-P-methyl-N-(2-oxo-1-propyl-1,2,3,4-tetra-hydroquinolin-6-yl)phosphinamidate **12 k***. 3,4-Dihydroquinolin-2(1H)-one (20.0 g, 136.05 mmol) was added to conc. sulfuric acid (200 ml) and cooled to −20 °C, and fuming nitric acid (4 ml, 95.24 mmol) was then added dropwise carefully over a period of 30 min. The resulting reaction mixture was stirred at −20 °C for 2 h and at room temperature for a further 2 h and then carefully diluted with ice-water. The aqueous phase was then repeatedly extracted with ethyl acetate. The combined organic phases were dried over magnesium sulfate, filtered and concentrated under reduced pressure. By column chromatography purification of the crude product obtained (ethyl acetate/heptane gradient), 6-nitro-3,4-dihydroquinolin-2(1H)-one (20.0 g, 76% of theory) was isolated as a colorless solid. 6-Nitro-3,4-dihydroquinolin-2(1H)-one (8.52 g, 44.38 mmol) was dissolved under argon in abs. *N,N*-dimethylformamide (150 ml), the mixture was cooled to 0 °C and fine potassium carbonate powder (7.40 g, 52.26 mmol) was added. After 15 min of stirring at a temperature of 0 °C, *n*-propyl iodide (2 equiv, 88.771 mmol) was added. The resulting reaction mixture was then stirred at room temperature for 24 h and, after cooling to room temperature, water and ethyl acetate were added. The aqueous phase was then repeatedly extracted with ethyl acetate. The combined organic phases were dried over magnesium sulfate, filtered and concentrated under reduced pressure. Column chromatography purification of the crude product obtained (ethyl acetate/heptane gradient) gave 6-nitro-1-propyl-3,4-dihydroquinolin-2(1H)-one (8.40 g, 87% of theory) as a colorless solid. In the next step, 6-nitro-1-propyl-3,4-dihydroquinolin-2(1H)-one (5.0 g, 24.27 mmol) was dissolved in an ethanol/water mixture (ratio 1:1, 50 ml), and ammonium chloride (12.96 g, 242.72 mmol) and iron powder (4.07 g, 72.82 mmol) were added. The resulting reaction mixture was stirred at a temperature of 80 °C for 2 h and, after cooling to room temperature, concentrated. Ethyl acetate and water were added to the residue and the aqueous phase was then repeatedly extracted with ethyl acetate. The combined organic phases were dried over magnesium sulfate, filtered and concentrated under reduced pressure. Column chromatography purification of the crude product obtained (ethyl acetate/heptane gradient) gave 6-amino-1-propyl-3,4-dihydroquinolin-2(1H)-one (4.0 g, 94% of theory) as a colorless solid. ^{1}H NMR (400 MHz, d_6-DSMO δ, ppm) 6.79 (d, 1H), 6.45 (m, 1H), 6.42 (m, 1H), 4.85 (br. s, 2H, NH_2), 3.75 (m, 2H), 2.68 (m, 2H), 2.43 (m, 2H), 1.52 (m, 2H), 0.85 (t, 3H). Methyldiethyl phosphite (1 equiv, 8.07 mmol) and benzyl bromide (1.54 ml, 8.07 mmol) were added to a multi-necked flask which had been dried by heating and then stirred together under continuous nitrogen flow at a temperature of 100 °C for 10 h. After complete conversion, without further purification, distilled $POCl_3$ (1 equiv) was added to the resulting crude product and the mixture was stirred under argon at a temperature of 60 °C for 1.5 h. After complete conversion, the benzyl(methyl)phosphine chloride obtained was, without further purification, directly reacted in the next step. Under argon, 6-amino-1-propyl-3,4-dihydroquinolin-2(1H)-one (1 equiv., 4.13 mmol) was dissolved together with benzyl(methyl)phosphine chloride (1 equiv., 4.13 mmol) in abs. tetrahydrofuran (10 ml) in a round-bottom flask which had been dried by heating, the mixture was cooled to a temperature of −20 °C, then triethylamine (1.2 ml, 8.26 mmol) was added and the mixture was stirred at room temperature for 2 h. The reaction mixture was then concentrated under reduced pressure, dil. HCl and dichloromethane were added to the residue that remained and the aqueous phase was extracted repeatedly with dichloromethane. The combined organic phases were dried over magnesium sulfate, filtered and concentrated under reduced pressure. Column chromatography purification of the crude product obtained (ethyl acetate/heptane gradient) gave *P*-benzyl-*P*-methyl-N-(2-oxo-1-propyl-1,2,3,4-tetrahydroquinolin-6-yl)phosphinamide **12 k** (103 mg, 7% of theory over three steps) as a colorless solid.[1] H-NMR (400 MHz, $CDCl_3$ δ, ppm) 7.37–7.26 (m, 6H), 6.83 (m, 1H), 6.61 (m, 1H), 6.45 (br. s, 1H, NH), 3.75 (m, 2H), 3.35–3.30 (m, 3H), 2.81 (m, 2H), 2.62 (m, 2H), 1.52 (m, 2H), 1.46 (m, 3H), 0.85 (t, 3H); LCMS (ESI, *m/z*): $[M]^+$ 356.4; HRMS (ESI, *m/z*): calcd. for $C_{20}H_{25}N_2O_2P$, 356.1654 $[M+H]^+$; found 356.1642.

*4.2.3. Preparation of phosphonamidates **13a-o***

All cpds were prepared following the protocols outlined for the syntheses of **13 g, 13 h, 13i, 13 l, 13n, 13o**.

*4.2.3.1. Methyl N-[1-(n-propyl)-2-oxo-1,2,3,4-tetrahydro-quinolin-6-yl]-P-(4-chlorobenzyl)phosphonamidate **13a**.*. White solid; yield 7%; ^{1}H NMR (400 MHz, $CDCl_3$ δ, ppm) 7.47 (m, 2H), 7.34 (m, 2H), 6.90 (m, 1H), 6.81 (m, 1H), 6.69 (m, 1H), 4.93 (br. s, 1H, NH), 3.87 (m, 2H),

3.73/3.68 (d, 3H), 3.27/3.02 (d, 2H), 2.83–2.78 (m, 2H), 2.64–2.58 (m, 2H), 1.70–1.61 (m, 2H), 0.98 (t, 3H); LCMS (ESI, *m/z*): $[M+H]^+$ 407.8; HRMS (ESI, *m/z*): calcd. for $C_{20}H_{24}N_2O_3PCl$, 406.8429 $[M]^+$; found 406.8444.

4.2.3.2. Methyl N-[1-(n-propyl)-2-oxo-1,2,3,4-tetrahydro-quinolin-6-yl]-P-(4-methylbenzyl)phosphonamidate ***13b***. White solid; yield 12%; ^{1}H NMR (400 MHz, $CDCl_3$ δ, ppm) 7.07–7.03 (m, 4H), 6.88 (m, 1H), 6.80 (m, 1H), 6.72 (m, 1H), 4.90 (br. s, 1H, NH), 3.87 (m, 2H), 3.75/3.69 (d, 3H), 3.26/3.05 (d, 2H), 2.83–2.78 (m, 2H), 2.65–2.60 (m, 2H), 2.32 (s, 3H), 1.71–1.63 (m, 2H), 0.96 (t, 3H); LCMS (ESI, *m/z*): $[M+H]^+$ 387.4.

4.2.3.3. Methyl N-[1-(n-propyl)-2-oxo-1,2,3,4-tetrahydro-quinolin-6-yl]-P-(4-fluorobenzyl)phosphonamidate ***13c***. White solid; yield 9%; ^{1}H NMR (400 MHz, $CDCl_3$ δ, ppm) 7.15 (m, 2H), 7.02 (m, 2H), 6.92 (m, 2H), 6.80 (m, 1H), 4.94 (br. s, 1H, NH), 3.87 (m, 2H), 3.71/3.65 (d, 3H), 3.24/3.04 (d, 2H), 2.83–2.78 (m, 2H), 2.65–2.60 (m, 2H), 1.71–1.63 (m, 2H), 0.96 (t, 3H); LCMS (ESI, *m/z*): $[M+H]^+$ 391.3.

4.2.3.4. Methyl N-[1-(n-propyl)-2-oxo-1,2,3,4-tetrahydro-quinolin-6-yl]-P-(4-cyanobenzyl)phosphonamidate ***13d***. White solid; yield 11%; ^{1}H NMR (400 MHz, $CDCl_3$ δ, ppm) 7.63 (m, 2H), 7.33 (m, 2H), 6.93 (m, 2H), 6.85 (m, 1H), 4.99 (br. s, 1H, NH), 3.87 (m, 2H), 3.73/3.68 (d, 3H), 3.27/3.02 (d, 2H), 2.83–2.78 (m, 2H), 2.64–2.58 (m, 2H), 1.70–1.61 (m, 2H), 0.98 (t, 3H); LCMS (ESI, *m/z*): $[M]^+$ 397.4.

4.2.3.5. Methyl N-[1-(methyl)-2-oxo-1,2,3,4-tetrahydroquino-lin-6-yl]-P-(4-methylbenzyl)phosphonamidate ***13e***. White solid; yield 15%; ^{1}H NMR (400 MHz, $CDCl_3$ δ, ppm) 7.08–7.03 (m, 4H), 6.87–6.79 (m, 2H), 6.72 (m, 1H), 5.14 (br. s, 1H, NH), 3.73/3.52 (d, 3H), 3.33 (s, 3H), 3.27/3.02 (d, 2H), 2.85–2.82 (m, 2H), 2.65–2.62 (m, 2H), 2.30 (s, 3H); LCMS (ESI, *m/z*): $[M+H]^+$ 359.4.

4.2.3.6. Methyl N-[1-(ethyl)-2-oxo-1,2,3,4-tetrahydroquinolin-6-yl]-P-(4-methylbenzyl)phosphonamidate ***13f***. White solid; yield 6%; ^{1}H NMR (400 MHz, $CDCl_3$ δ, ppm) 7.12–7.00 (m, 4H), 6.89 (m, 1H), 6.81 (m, 1H), 6.70 (m, 1H), 5.08 (br. s, 1H, NH), 3.97–3.92 (m, 2H), 3.75 (d, 3H), 3.43/3.23 (d, 2H), 2.83–2.78 (m, 2H), 2.63–2.58 (m, 2H), 2.30 (s, 3H), 1.26–1.22 (t, 3H). LCMS (ESI, *m/z*): $[M]^+$ 373.2. HRMS (ESI, *m/z*): calcd. for $C_{20}H_{25}N_2O_3P$, 372.3979 $[M]^+$; found 372.3967.

4.2.3.7. Methyl N-[1-(cyclopropylmethyl)-2-oxo-1,2,3,4-tetrahydroquinolin-6-yl]-P-(4-methylbenzyl)phosphonamidate ***13g***. 3,4-Dihydroquinolin-2(1H)-one (770 mg, 3.83 mmol) was added to conc. acetic acid (5 ml), and fuming nitric acid (0.21 ml, 5.06 mmol) was then added carefully. The resulting reaction mixture was stirred at room temperature for 2 h and then diluted with ice-water. The aqueous phase was then repeatedly extracted with ethyl acetate. The combined organic phases were dried over magnesium sulfate, filtered and concentrated under reduced pressure. By column chromatography purification of the crude product obtained (ethyl acetate/heptane gradient), 6-nitro-3,4-dihydroquinolin-2(1H)-one (500 mg, 68% of theory) was isolated as a colorless solid. 6-Nitro-3,4-dihydroquinolin-2(1H)-one (500 mg, 2.60 mmol) was dissolved under argon in abs. N,*N*-dimethylformamide and admixed with fine potassium carbonate powder (1.08 mg, 7.81 mmol). After stirring at room temperature for 5 min, chloromethylcyclopropane (306 mg, 3.38 mmol) and potassium iodide (6 mg, 0.04 mmol) were added. The resulting reaction mixture was stirred at 120 °C for 2 h and, after cooling to room temperature, water and ethyl acetate were added. The aqueous phase was then repeatedly extracted with ethyl acetate. The combined organic phases were dried over magnesium sulfate, filtered and concentrated under reduced pressure. By column chromatography purification of the crude product obtained (ethyl acetate/heptane gradient), 1-(cyclopropylmethyl)-6-nitro-3,4-dihydroquinolin-2(1H)-one (600 mg, 94% of theory) was isolated as a colorless solid. ^{1}H NMR (400 MHz, $CDCl_3$ δ, ppm) 8.17 (dd, 1H), 8.08 (d, 1H), 7.22 (d, 1H), 3.91 (d, 2H), 3.04 (m, 2H), 2.73 (m, 2H), 1.12 (m, 1H), 0.55 (m, 2H), 0.45 (m, 2H). In the next step, 1-(cyclopropylmethyl)-6-nitro-3,4-dihydroquinolin-2(1H)-one (600 mg, 2.44 mmol) was added together with tin(II) chloride dihydrate (2.19 g, 9.75 mmol) to abs. ethanol and the mixture was stirred under argon at a temperature of 80 °C for 5 h. After cooling to room temperature, the reaction mixture was poured into ice-water and then adjusted to pH 12 with aqueous NaOH. The aqueous phase was then repeatedly extracted with ethyl acetate. The combined organic phases were dried over magnesium sulfate, filtered and concentrated under reduced pressure. By column chromatography purification of the crude product obtained (ethyl acetate/heptane gradient), 6-amino-1-(cyclopropylmethyl)-3,4-dihydroquinolin-2(1H)-one (481 mg, 91% of theory) was isolated as a colorless solid. ^{1}H NMR (400 MHz, $CDCl_3$ δ, ppm) 6.94 (d, 1H), 6.58 (dd, 1H), 6.53 (d, 1H), 3.83 (d, 3H), 2.81 (m, 2H), 2.61 (m, 2H), 1.12 (m, 1H), 0.47 (m, 2H), 0.39 (m, 2H). Trimethyl phosphite (1 equiv, 8.07 mmol) and 4-methylbenzyl bromide (1 equiv, 8.07 mmol) were added to a multi-necked flask which had been dried by heating and then stirred together under continuous nitrogen flow at a temperature of 100 °C for 10 h. After complete conversion, without further purification, distilled $POCl_3$ (1 equiv) was added to the resulting crude product and the mixture was stirred under argon at a temperature of 60 °C for 1.5 h. After complete conversion, the methyl (4-methylbenzyl)phosphono-chloridate obtained was, without further purification, directly reacted in the next step. In a round-bottom flask which had been dried by heating, under argon, 6-amino-1-cyclopropylmethyl-3,4-dihydroquinolin-2(1H)-one (960 mg, 4.57 mmol) was dissolved in abs. tetrahydrofuran (2 ml) and slowly added dropwise under argon to a solution, cooled to −20 °C, of methyl (4-methylbenzyl)-phosphonochloridate (1000 mg, 4.57 mmol) in abs. tetrahydrofuran (10 ml) in a round-bottom flask which had been dried beforehand by heating. The resulting reaction mixture was stirred at −20 °C for 10 min, triethylamine (1.27 ml, 9.15 mmol) was then added and the mixture was subsequently stirred at room temperature for 2 h. The reaction mixture was then filtered, the filter cake was washed with tetrahydrofuran and the filtrate was concentrated under reduced pressure. By column chromatography purification of the crude product obtained (ethyl acetate/heptane gradient), methyl N-[1-(cyclopropylmethyl)-2-oxo-1,2,3,4-tetrahydroquinolin-6-yl]-P-(4-methylbenzyl)-phos-phonamidate **13 g** (209 mg, 10% of theory) was isolated as a colorless solid. ^{1}H NMR (400 MHz, $CDCl_3$ δ, ppm) 7.09–7.04 (m, 4H), 7.02 (m, 1H), 6.83 (m, 1H), 6.73 (m, 1H), 5.01 (br. s, 1H, NH), 3.84 (d, 2H), 3.76 / 3.53 (d, 3H), 3.25/3.00 (d, 2H), 2.87–2.82 (m, 2H), 2.65–2.61 (m, 2H), 2.32/2.30 (s, 3H), 1.13 (m, 1H), 0.53–0.48 (m, 2H), 0.45–0.41 (m, 2H); ^{13}C NMR (150 MHz, $CDCl_3$ δ, ppm) 170.3, 141.4, 138.9, 134.3, 133.8, 130.0, 129.4, 129.2, 128.4, 128.2, 123.8, 117.0, 116.1, 53.7, 48.2, 32.9, 28.8, 25.2, 23.6, 21.5, 7.6, 7.2; LCMS (ESI, *m/z*): $[M]^+$ 398.2; HRMS (ESI, *m/z*): calcd. for $C_{22}H_{27}N_2O_3P$, 398.4351 $[M]^+$; found 398.4338.

4.2.3.8. Methyl N-{1-[1,1′-bi(cyclopropyl)-1-yl]-2-oxo-1,2,3,4-tetrahydro quinolin-6-yl}-P-(4-methylphenyl)-phosphon-amidate ***13 h***. Ethyl (2E)-3-(2-fluoro-5-nitrophenyl)acrylate (1000 mg, 4.18 mmol) and 1,1′-bi(cyclopropyl)-1-amine (508 mg, 3.80 mmol) were dissolved under argon in abs. N,*N*-dimethylformamide (10 ml), and then N,*N*-diisopropylethylamine (1.32 ml, 7.60 mmol) was added. The resulting reaction mixture was stirred at a temperature of 50 °C for a total of 16 h and, after cooling to room temperature, water and ethyl acetate were added. The aqueous phase was then extracted repeatedly with ethyl acetate. The combined organic phases were dried over magnesium sulfate, filtered and concentrated under reduced pressure. Column chromatography purification of the crude product obtained (ethyl acetate/heptane gradient) gave ethyl (2E)-3-{2-[1,1′-bi(cyclopropyl)-1-ylamino]-5-nitrophenyl}acrylate (570 mg, 43% of theory) as a colorless solid, ^{1}H NMR (400 MHz, $CDCl_3$ δ, ppm) 8.27 (d, 1H), 8.16 (m, 1H), 7.63 (d, 1H), 7.18 (d, 1H), 6.46 (d, 1H), 5.19 (br. s, 1H, NH), 4.29 (q, 2H), 1.35 (t, 3H), 1.33–1.27 (m, 1H), 0.78 (m, 4H), 0.49 (m, 2H), 0.18 (m, 2H). Ethyl (2E)-3-{2-[1,1′-bi(cyclopropyl)-1-ylamino]-5-nitrophenyl}acrylate (570 mg, 1.80 mmol) was then dissolved in abs.

ethanol (10 ml), and $(Ph_3P)_3RhCl$ (167 mg, 0.18 mmol) was added. After stirring at room temperature for 5 min, hydrogen was introduced into the reaction solution with a constant gas flow via a gas introduction apparatus for about 9 h. The progress of the reaction was monitored by LC-MS. On completion of conversion, the reaction solution was concentrated under reduced pressure. Column chromatography purification of the crude product obtained (ethyl acetate/heptane gradient) gave ethyl 3-{2-[1,1′-bi(cyclopropyl)-1-ylamino]-5-nitrophenyl}propanoate (200 mg, 35% of theory) as a colorless solid, ^{1}H NMR (400 MHz, $CDCl_3$ δ, ppm) 8.07 (m, 1H), 7.94 (d, 1H), 7.11 (d, 1H), 5.40 (br. s, 1H, NH), 4.18 (q, 2H), 2.77 (m, 2H), 2.64 (m, 2H), 1.30–1.24 (m, 4H), 0.76 (m, 4H), 0.46 (m, 2H), 0.17 (m, 2H). Ethyl 3-{2-[1,1′-bi(cyclopropyl)-1-ylamino]-5-nitrophenyl} propanoate (200 mg, 0.63 mmol) was dissolved in abs. tetrahydrofuran (8 ml) and, under argon, added dropwise to a suspension, cooled to 0 °C, of sodium hydride (38 mg, 0.94 mmol, 60% suspension in oil) in abs. tetrahydrofuran (5 ml). The resulting reaction mixture was stirred at 0 °C for 1 h, and then water was added cautiously, followed by ethyl acetate after stirring for 5 min. The aqueous phase was then extracted repeatedly with ethyl acetate. The combined organic phases were dried over magnesium sulfate, filtered and concentrated under reduced pressure. Column chromatography purification of the crude product obtained (ethyl acetate/heptane gradient) gave 1-[1,1′-bi(cyclopropyl)-1-yl]-6-nitro-3,4-dihydro quinolin-2(1H)-one (90 mg, 53%) as a colorless solid, ^{1}H NMR (400 MHz, $CDCl_3$ δ, ppm) 8.16 (m, 1H), 8.04 (m, 1H), 7.53 (d, 1H), 2.93 (m, 2H), 2.78–2.58 (m, 2H), 1.44 (m, 1H), 1.23 (m, 1H), 1.03 (m, 1H), 0.91–0.82 (m, 2H), 0.60–0.45 (m, 3H), 0.28 (m, 1H). In the next step, 1-[1,1′-bi(cyclopropyl)-1-yl]-6-nitro-3,4-dihydroquinolin-2(1H)-one (90 mg, 0.33 mmol) was, together with tin(II) chloride dihydrate (298 mg, 1.32 mmol), added to abs. ethanol (5 ml) and stirred under argon at a temperature of 80 °C for 5 h. After cooling to room temperature, the reaction mixture was poured into ice-water and then adjusted to pH 12 with aqueous NaOH. The aqueous phase was then extracted repeatedly with ethyl acetate. The combined organic phases were dried over magnesium sulfate, filtered and concentrated under reduced pressure. Column chromatography purification of the crude product obtained (ethyl acetate/heptane gradient) gave 6-amino-1-[1,1′-bi(cyclopropyl)-1-yl]-3,4-dihydroquinolin-2(1H)-one (70 mg, 87% of theory) as a highly viscous foam, ^{1}H NMR (400 MHz, $CDCl_3$ δ, ppm) 7.18 (m, 1H), 6.58 (m, 1H), 6.48 (d, 1H), 2.78 (m, 2H), 2.59 (m, 2H), 1.47 (m, 1H), 1.08 (m, 1H), 0.98 (m, 1H), 0.90–0.81 (m, 2H), 0.60–0.43 (m, 3H), 0.28 (m, 1H). Trimethyl phosphite (1 equiv, 8.07 mmol) and 4-methylbenzyl bromide (1 equiv, 8.07 mmol) were added to a multi-necked flask which had been dried by heating and then stirred together under continuous nitrogen flow at a temperature of 100 °C for 10 h. After complete conversion, without further purification, distilled $POCl_3$ (1 equiv) was added to the resulting crude product and the mixture was stirred under argon at a temperature of 60 °C for 1.5 h. After complete conversion, the methyl (4-methylbenzyl)phosphonochloridate obtained was, without further purification, directly reacted in the next step. In a round-bottom flask which had been dried by heating, under argon, 6-amino-1-[1,1′-bi (cyclopropyl)-1-yl]-3,4-dihydro-quinolin-2(1H)-one (1108 mg, 4.57 mmol) was dissolved in abs. tetrahydrofuran (2 ml) and slowly added dropwise under argon to a solution, cooled to −20 °C, of methyl (4-methylbenzyl)phosphonochloridate (1000 mg, 4.57 mmol) in abs. tetrahydrofuran (10 ml) in a round-bottom flask which had been dried beforehand by heating. The resulting reaction mixture was stirred at −20 °C for 10 min, triethylamine (1.27 ml, 9.15 mmol) was then added and the mixture was subsequently stirred at room temperature for 2 h. The reaction mixture was then filtered, the filter cake was washed with tetrahydrofuran and the filtrate was concentrated under reduced pressure. Column chromatography purification of the crude product obtained (ethyl acetate/heptane gradient), gave methyl N-{1-[1,1′-bi (cyclopropyl)-1-yl]-2-oxo-1,2,3,4-tetrahydroquinolin-6-yl}-P-(4-methylphenyl)phosphonamidate ***13 h*** (243 mg, 11% of theory) as a colorless solid.[1] ^{1}H-NMR (400 MHz, $CDCl_3$ δ, ppm) 7.28–7.22 (m, 2H), 7.13 (m, 1H), 7.10–7.04 (m, 2H), 6.81 (m, 1H), 6.68 (m, 1H), 5.11 (br. s, 1H, NH), 3.72/3.52 (d, 3H), 3.30–2.90 (m, 2H), 3.25/3.00 (d, 2H), 2.82–2.53 (m, 2H), 2.32/2.27 (s, 3H), 1.47 (m, 1H), 1.09 (m, 1H), 0.99 (m, 1H), 0.78–0.70 (m, 1H), 0.59–0.42 (m, 4H), 0.27 (m, 1H). LCMS (ESI, *m/z*): $[M]^+$ 424.5; HRMS (ESI, *m/z*): calcd. for $C_{24}H_{29}N_2O_3P$, 424.1916 $[M]^+$; found 424.1929.

4.2.3.9. Methyl N-[2-oxo-1-(spiro[3.3]hept-2-yl)-1,2,3,4-tetrahydroquinolin-6-yl]-P-(4-methylphenyl)phosphonamidate ***13i.*** Ethyl (2E)-3-(2-fluoro-5-nitrophenyl)acrylate (1000 mg, 4.18 mmol) and spiro[3.3]hept-2-ylamine (561 mg, 3.80 mmol) were dissolved under argon in abs. N,*N*-dimethylformamide, and then N,*N*-diisopropylethylamine (1.32 ml, 7.60 mmol) was added. The resulting reaction mixture was stirred at a temperature of 50 °C for 10 h and, after cooling to room temperature, water and ethyl acetate were added. The aqueous phase was then extracted repeatedly with ethyl acetate. The combined organic phases were dried over magnesium sulfate, filtered and concentrated under reduced pressure. Column chromatography purification of the crude product obtained (ethyl acetate/heptane gradient) gave ethyl (2E)-3-[5-nitro-2-(spiro[3.3]hept-2-ylamino)phenyl]acrylate (500 mg, 36% of theory) as a colorless solid, ^{1}H NMR (400 MHz, $CDCl_3$ δ, ppm) 8.26 (d, 1H), 8.11 (m, 1H), 7.67 (d, 1H), 6.51 (m, 1H), 6.47 (d, 1H), 4.82 (br. m, 1H, NH), 4.29 (q, 2H), 3.88 (m, 1H), 2.60 (m, 2H), 2.12 (m, 2H), 2.01 (m, 2H), 1.95–1.85 (m, 4H), 1.37 (t, 3H). Ethyl (2E)-3-[5-nitro-2-(spiro[3.3] hept-2-ylamino)phenyl]acrylate (500 mg, 1.51 mmol) was then dissolved in abs. ethanol (8 ml), and $(Ph_3P)_3RhCl$ (70 mg) was added. After stirring at room temperature for 5 min, hydrogen was introduced into the reaction solution with a constant gas flow via a gas introduction apparatus for 10 h. The progress of the reaction was monitored by LCMS. On completion of conversion, the reaction solution was concentrated under reduced pressure. Column chromatography purification of the crude product obtained (ethyl acetate/heptane gradient) gave ethyl 3-[5-nitro-2-(spiro [3.3]hept-2-ylamino)phenyl]propanoate (490 mg, 97% of theory) as a colorless solid, ^{1}H NMR (400 MHz, $CDCl_3$ δ, ppm) 8.04 (dd, 1H), 7.94 (d, 1H), 6.43 (d, 1H), 5.11 (br. m, 1H, NH), 4.28 (q, 2H), 3.87 (m, 1H), 2.81 (m, 2H), 2.67 (m, 2H), 2.58 (m, 2H), 2.11 (m, 2H), 2.00 (m, 2H), 1.92–1.85 (m, 4H), 1.28 (t, 3H). Ethyl 3-[5-nitro-2-(spiro[3.3]hept-2-ylamino)phenyl]propanoate (490 mg, 1.47 mmol) was dissolved in abs. tetrahydrofuran (8 ml) and, under argon, added dropwise to a suspension, cooled to 0 °C, of sodium hydride (88 mg, 2.21 mmol, 60% suspension in oil) in abs. tetrahydrofuran (5 ml). The resulting reaction mixture was stirred at 0 °C for 1 h, and then water was added cautiously, followed by ethyl acetate after stirring for 5 min. The aqueous phase was then extracted repeatedly with ethyl acetate. The combined organic phases were dried over magnesium sulfate, filtered and concentrated under reduced pressure. Column chromatography purification of the crude product obtained (ethyl acetate/heptane gradient) gave 6-nitro-1-(spiro [3.3]hept-2-yl)-3,4-dihydroquinolin-2(1H)-one (180 mg, 43%) as a colorless solid, ^{1}H NMR (400 MHz, $CDCl_3$ δ, ppm) 8.11–8.07 (m, 2H), 6.84 (d, 1H), 4.29 (m, 1H), 2.92 (m, 2H), 2.74 (m, 2H), 2.61 (m, 2H), 2.12 (m, 2H), 2.07 (m, 2H), 1.94–1.83 (m, 4H). In the next step, 6-nitro-1-(spiro [3.3]hept-2-yl)-3,4-dihydroquinolin-2(1H)-one (180 mg, 2.44 mmol) was, together with tin(II) chloride dihydrate (567 mg, 2.52 mmol), added to abs. ethanol and stirred under argon at a temperature of 80 °C for 5 h. After cooling to room temperature, the reaction mixture was poured into ice-water and then adjusted to pH 12 with aqueous NaOH. The aqueous phase was then extracted repeatedly with ethyl acetate. The combined organic phases were dried over magnesium sulfate, filtered and concentrated under reduced pressure. Column chromatography purification of the crude product obtained (ethyl acetate/heptane gradient) gave 6-amino-1-(spiro[3.3]hept-2-yl)-3,4-dihydroquinolin-2(1H)-one (151 mg, 94% of theory) as a highly viscous foam, ^{1}H NMR (400 MHz, $CDCl_3$ δ, ppm) 6.59–6.53 (m, 3H), 4.32–3.80 (br. s, 2H, NH_2), 4.21 (m, 1H), 2.72 (m, 2H), 2.67 (m, 2H), 2.48 (m, 2H), 2.12–2.06 (m,

4H), 1.93–1.80 (m, 4H). Trimethyl phosphite (1 equiv, 8.07 mmol) and 4-methylbenzyl bromide (1 equiv, 8.07 mmol) were added to a multi-necked flask which have been dried by heating and then stirred together under continuous nitrogen flow at a temperature of 100 °C for 10 h. After complete conversion, a partial amount of the resulting crude product (170 mg) was, without further purification, taken up in aqueous NaOH (10% strength, 5 ml), and the mixture was stirred under reflux conditions for 2 h. After cooling to room temperature, dil. hydrochloric acid was added carefully, followed by thorough extraction with dichloromethane and water. The combined organic phases were dried over magnesium sulfate, filtered and concentrated under reduced pressure. Without further purification, the resulting crude product (109 mg, 0.54 mmol) was initially charged into abs. N,*N*-dimethylformamide (2 ml) and cooled to 0 °C. After 5 min of stirring at 0 °C, oxalyl chloride (0.12 ml, 1.63 mmol) was added and the reaction mixture obtained was stirred at room temperature for one and a half hours and then concentrated under reduced pressure. The resulting methyl (4-methylbenzyl)-phosphonochloridate was taken up in abs. dichloromethane (5 ml) and cooled to a temperature of −20 °C, and a solution of 6-amino-1-(spiro[3.3]hept-2-yl)-3,4-dihydro-quinolin-2(1H)-one (167 mg, 0.65 mmol) mmol) in abs. dichloromethane (2 ml) was added. This was followed by the dropwise addition of *N*-ethyldiisopropylamine (0.17 ml, 1.19 mmol). The resulting reaction mixture was stirred at −20 °C for 10 min and then at room temperature for 2 h. The reaction mixture was then filtered, the filter cake was washed with dichloromethane and the filtrate was concentrated under reduced pressure. Column chromatography purification of the crude product obtained (ethyl acetate/heptane gradient) gave methyl N-[2-oxo-1-(spiro[3.3]hept-2-yl)-1,2,3,4-tetrahydroquinolin-6-yl]-P-(4-methylphenyl) phosphonamidate **13i** (10 mg, 4% of theory) as a highly viscous foam. ^{1}H NMR (400 MHz, $CDCl_3$ δ, ppm) 7.15–7.11 (m, 2H), 7.09–7.05 (m, 2H), 6.99 (m, 1H), 6.83 (m, 1H), 6.68–6.65 (m, 1H), 5.15 (br. s, 1H, NH), 4.24–4.19 (m, 1H), 3.65/3.43 (m, 3H), 3.14/3.03 (d, 2H), 2.73–2.69 (m, 2H), 2.67–2.63 (m, 2H), 2.52–2.46 (m, 2H), 2.32 (s, 3H), 2.15–2.03 (m, 4H), 1.85–1.70 (m, 4H). LCMS (ESI, *m/z*): $[M]^+$ 438.5

*4.2.3.10. Methyl N-[1-methyl-2-oxo-1,2,3,4-tetrahydro-quinolin-6-yl]-P-(4-chlorobenzyl)phosphonamidate **13j**.*. White solid; yield 5%; ^{1}H NMR (400 MHz, $CDCl_3$ δ, ppm) 7.47 (m, 2H), 7.34 (m, 2H), 6.90 (m, 1H), 6.81 (m, 1H), 6.69 (m, 1H), 4.93 (br. s, 1H, NH), 3.87 (m, 2H), 3.73/3.68 (d, 3H), 3.29 (s, 3H), 3.25/3.04 (d, 2H), 2.83–2.78 (m, 2H), 2.64–2.58 (m, 2H); LCMS (ESI, *m/z*): $[M+H]^+$ 379.7.

*4.2.3.11. Methyl N-[1-(n-propyl)-2-oxo-1,2,3,4-tetrahydro-quinolin-6-yl]-P-(3-chlorobenzyl)phosphonamidate **13 k**.*. White solid; yield 7%; ^{1}H NMR (400 MHz, $CDCl_3$ δ, ppm) 7.32 (m, 1H), 7.06–6.95 (m, 2H), 6.91–6.81 (m, 2H), 6.69 (m, 1H), 4.98 (br. s, 1H, NH), 3.87 (m, 2H), 3.73/3.68 (d, 3H), 3.27/3.02 (d, 2H), 2.83–2.78 (m, 2H), 2.64–2.58 (m, 2H), 1.70–1.61 (m, 2H), 0.98 (t, 3H); LCMS (ESI, *m/z*): $[M+H]^+$ 407.8.

*4.2.3.12. Ethyl N-[1-(n-propyl)-2-oxo-1,2,3,4-tetrahydro-quinolin-6-yl]-P-(4-methylbenzyl)phosphonamidate **13 l**.*. Triethyl phosphite (2.00 g, 12.04 mmol) and 4-methylbenzyl bromide (15.65 mmol) were added to a microwave vessel which had been dried by heating and then stirred together in the microwave under nitrogen at a temperature of 140 °C for 1 h. After complete conversion, the resulting crude product was purified by column chromatography (heptane/ethyl acetate gradient), distilled $POCl_3$ (4.43 mmol) was then added to a partial amount of the resulting purified intermediate (4.43 mmol) and the mixture was stirred under argon at a temperature of 60 °C for 1.5 h. After complete conversion, the reaction mixture was concentrated carefully and the ethyl (4-methylbenzyl)phosphonochloridate obtained was, without further purification, directly reacted in the next step. In a round-bottom flask which had been dried by heating, under argon, 6-amino-1-propyl-3,4-dihydroquinolin-2(1H)-one (904 mg, 4.43 mmol) was dissolved in abs. tetrahydrofuran (2 ml) and slowly added dropwise under argon to a solution, cooled to −20 °C, of ethyl (4-ethylbenzyl) phosphonochloridate (1030 mg, 4.43 mmol) in abs. tetrahydrofuran (8 ml) in a round-bottom flask which had been dried beforehand by heating. The resulting reaction mixture was stirred at −20 °C for 10 min, triethylamine (1.23 ml, 8.86 mmol) was then added and the mixture was subsequently stirred at room temperature for 2 h. The reaction mixture was then filtered, the filter cake was washed with tetrahydrofuran and the filtrate was concentrated under reduced pressure. Column chromatography purification of the crude product obtained (ethyl acetate/heptane gradient) gave ethyl N-[1-(*n*-propylmethyl)-2-oxo-1,2,3,4-tetrahydroquinolin-6-yl]-P-(4-methylbenzyl)phosphonamidate **13 l** (224 mg, 12% of theory) as a colourless solid. ^{1}H NMR (600 MHz, $CDCl_3$ δ, ppm) 7.16–03 (m, 4H), 6.87 (m, 1H), 6.81 (m, 1H), 6.72 (m, 1H), 5.00 (br. m, 1H, NH), 4.24–4.17 (m, 1H), 4.08–4.00 (m, 1H), 3.90–3.84 (m, 2H), 3.27/3.02 (d, 2H), 2.83–2.78 (m, 2H), 2.63–2.59 (m, 2H), 2.30 (s, 3H), 1.71–1.63 (m, 2H), 1.33 (t, 3H), 0.96 (t, 3H); LCMS (ESI, *m/z*): $[M]^+$ 400.2; logp 2.44.

*4.2.3.13. Ethyl N-[1-(n-propyl)-2-oxo-1,2,3,4-tetrahydro-quinolin-6-yl]-P-(4-chlorobenzyl)phosphonamidate **13 m**.*. White solid; yield 9%; ^{1}H NMR (400 MHz, $CDCl_3$ δ, ppm) 7.47 (m, 2H), 7.34 (m, 2H), 6.90 (m, 1H), 6.81 (m, 1H), 6.70 (m, 1H), 5.02 (br. m, 1H, NH), 4.24–4.17 (m, 1H), 4.08–4.00 (m, 1H), 3.90–3.84 (m, 2H), 3.27/3.02 (d, 2H), 2.83–2.78 (m, 2H), 2.63–2.59 (m, 2H), 2.30 (s, 3H), 1.71–1.63 (m, 2H), 1.33 (t, 3H), 0.96 (t, 3H); LCMS (ESI, *m/z*): $[M]^+$ 420.9

*4.2.3.14. Ethyl N-[1-(cyclopropylmethyl)-2-oxo-1,2,3,4-tetrahydroquinolin-6-yl]-P-(4-methylbenzyl)phosphonamidate **13n**.*. Triethyl phosphite (1 equiv, 8.07 mmol) and 4-methylbenzyl bromide (1 equiv, 8.07 mmol) were added to a multi-necked flask which had been dried by heating and then stirred together under continuous nitrogen flow at a temperature of 100 °C for 10 h. After complete conversion, without further purification, distilled $POCl_3$ (1 equiv) was added to the resulting crude product and the mixture was stirred under argon at a temperature of 60 °C for 1.5 h. After complete conversion, the ethyl (4-methylbenzyl)-phosphonochloridate obtained was, without further purification, directly reacted in the next step. In a round-bottom flask which had been dried by heating, under argon, 6-amino-1-cyclopropylmethyl-3,4-dihydroquinolin-2(1H)-one (890 mg, 4.11 mmol) was dissolved in abs. tetrahydrofuran (2 ml) and slowly added dropwise under argon to a solution, cooled to −20 °C, of ethyl (4-methylbenzyl)phosphonochloridate (957 mg, 4.11 mmol) in abs. tetrahydrofuran (8 ml) in a round-bottom flask which had been dried beforehand by heating. The resulting reaction mixture was stirred at −20 °C for 10 min, triethylamine (1.15 ml, 8.23 mmol) was then added and the mixture was subsequently stirred at room temperature for 2 h. The reaction mixture was then filtered, the filter cake was washed with tetrahydrofuran and the filtrate was concentrated under reduced pressure. By column chromatography purification of the crude product obtained (ethyl acetate/heptane gradient), ethyl N-[1-(cyclopropylmethyl)-2-oxo-1,2,3,4-tetrahydroquinolin-6-yl]-P-(4-methylbenzyl)phosphonamidate **13n** (236 mg, 9% of theory) was isolated as a colorless solid. ^{1}H NMR (400 MHz, $CDCl_3$ δ, ppm) 7.17–7.03 (m, 4H), 7.00 (m, 1H), 6.83 (m, 1H), 6.72 (m, 1H), 5.03 (br. m, 1H, NH), 4.24–4.19 (m, 1H), 4.12–4.01 (m, 1H), 3.87 (m, 2H), 3.27/3.02 (d, 2H), 2.87–2.82 (m, 2H), 2.65–2.61 (m, 2H), 2.32/2.30 (s, 3H), 1.33 (t, 3H), 1.13 (m, 1H), 0.53–0.48 (m, 2H), 0.45–0.39 (m, 2H).; LCMS (ESI, *m/z*): $[M]^+$ 412.2; logp 2.59.

*4.2.3.15. Ethyl N-{1-[1,1′-bi(cyclopropyl)-1-yl]-2-oxo-1,2,3,4-tetrahydro quinolin-6-yl}-P-(4-methylphenyl)phosphonamidate **13o**.* Triethyl phosphite (1 equiv, 8.07 mmol) and 4-methylbenzyl bromide (1 equiv, 8.07 mmol) were added to a multi-necked flask which had been dried by heating and then stirred together under continuous nitrogen flow at a temperature of 100 °C for 10 h. After complete conversion, without further purification, distilled $POCl_3$ (1 equiv) was added to the resulting crude product and the mixture was stirred under argon at a temperature of 60 °C for 1.5 h. After complete conversion, the ethyl (4-methylbenzyl)-phosphonochloridate

obtained was, without further purification, directly reacted in the next step. In a round-bottom flask which had been dried by heating, under argon, 6-amino-1-[1,1′-bi(cyclopropyl)-1-yl]-3,4-dihydroquino-lin-2(1H)-one (1042 mg, 4.29 mmol) was dissolved in abs. tetrahydrofuran (2 ml) and slowly added dropwise under argon to a solution, cooled to −20 °C, of ethyl (4-methylbenzyl)phosphonochloridate (1000 mg, 4.29 mmol) in abs. tetrahydrofuran (10 ml) in a round-bottom flask which had been dried beforehand by heating. The resulting reaction mixture was stirred at −20 °C for 10 min, triethylamine (1.19 ml, 8.54 mmol) was then added and the mixture was subsequently stirred at room temperature for 2 h. The reaction mixture was then filtered, the filter cake was washed with tetrahydrofuran and the filtrate was concentrated under reduced pressure. Column chromatography purification of the crude product obtained (ethyl acetate/heptane gradient) gave ethyl N-{1-[1,1′-bi(cyclopropyl)-1-yl]-2-oxo-1,2,3,4-tetrahydro-quinolin-6-yl}-P-(4-methyl-phenyl) phosphonamidate **13o** (196 mg, 9% of theory) as a colourless solid. ^{1}H NMR (400 MHz, $CDCl_3$ δ, ppm) 7.28–7.23 (m, 2H), 7.13 (m, 1H), 7.11–7.02 (m, 2H), 6.82 (m, 1H), 6.68 (m, 1H), 5.04–4.91 (br. s, 1H, NH), 4.23–3.78 (m, 4H), 3.25/3.00 (d, 2H), 2.86–2.58 (m, 2H), 2.31/2.28 (s, 3H), 1.47 (m, 1H), 1.33/1.22 (m, 3H), 1.09 (m, 1H), 0.99 (m, 1H), 0.78–0.70 (m, 1H), 0.59–0.42 (m, 4H), 0.27 (m, 1H). LCMS (ESI, *m/z*): $[M]^+$ 438.4.

4.3. X-ray crystallography and modelling studies

4.3.1. X-ray crystallography

For structural studies AtRCAR11 and an *N*-terminally truncated version of AtHAB1 lacking residues 1–178 (ΔNAtHAB1) were used. Expression and purification were carried out according to published protocols.[50] The ternary complex between AtRCAR11, ΔNAtHAB1 and **6b** was obtained by mixing the components in 20 mM Tris pH 7.5, 150 mM NaCl, 1 mm $MnCl_2$, and 1 mm β-mercaptoethanol to final concentrations of 3 mg/ml, 5 mg/ml and 1 mM, respectively. Crystals of the complex were grown from 20% Peg 8000, 100 mM Tris pH 8.5, 160 mM $MgCl_2$, 60 mM glycylglycylglycine at 18 °C by sitting drop vapor diffusion. The crystals were transferred to crystallization solution supplemented with 25% glycerol as cryo-protectant and flash cooled in liquid nitrogen before data collection on an Xcalibur Nova diffraction system from Oxford Diffraction. The structures were solved by molecular replacement with MOLREP[51] using the ternary complex of RCAR11, ΔNHAB1 and ABA (pdb accession code 3QN1) as a search model. Manual model building and refinement were iteratively performed with Coot52 and RefMac5.[53] Data collection and refinement statistics are shown in Table S1.

4.3.2. Modelling studies

Modelling was done using the crystal structure of ABA-bound *At*RCAR11 with related phosphatase *At*HAB1 (3QN1 – F. Dupeux et al.).[50] Docking poses were generated using SeeSAR from BioSolveIT and scored using the HYDE scoring function.[43]

Declaration of Competing Interest

The authors declare that they have no known competing financial interests or personal relationships that could have appeared to influence the work reported in this paper.

Acknowledgements

We would like to thank Matthias Jank, Susanne Ries, Gudrun Fey, Peter Zöllner and Martin Annau for valuable analytical support. We would like to thank Sanjay Bhavsar for preparing some of the target compounds. Furthermore, we would like to thank David Barber for fruitful discussions during the preparation of the manuscript.

Appendix A. Supplementary data

Supplementary data to this article can be found online at https://doi.org/10.1016/j.bmc.2020.115725.

References

1. Li D, Luong TTM, Dan W-J, et al. *Bioorg. Med. Chem.* 2018;26:386.
2. S. Y. Salehi-Lisar, H. Bakhshayeshan-Agdam in Drought Stress Tolerance in Plants, Vol 1; Physiology and Biochemistry (Eds.: M. A. Hossain, S. H. Wani, S. Bhattacharjee, D. J. Burritt, L.-S. P. Tran), Springer-Verlag, Berlin Heidelberg, 2016, pp. 1-16.
3. Battisti DS, Naylor RL. *Science.* 2009;323:240.
4. Campos H, Cooper M, Habben JE, Edmeades GO, Schussler JR. *Field Crops Res.* 2004;90:19.
5. Nemali KS, Bonin C, Dohlemann FG, et al. *Plant Cell Environ.* 1866;2015:38.
6. Addicott FT, Lyon JL. *Annu. Rev. Plant Physiol.* 1969;20:139.
7. Milborrow BV. *Annu. Rev. Plant Physiol.* 1974;25:259.
8. Cutler SR, Rodriguez PL, Finkelstein RR, Abrams SR. *Annu. Rev. Plant Biol.* 2010;61:651.
9. Nambara E, Marion-Poll A. *Annu. Rev. Plant Biol.* 2005;56:165.
10. Yang Z, Liu J, Poree F, et al. *Plant Phys.* 2019;180:1066.
11. Ma Y, Szostkiewicz I, Korte A, et al. *Science.* 2009;324:1064.
12. Park S-Y, Fung P, Fung P, et al. *Science.* 2009;324:1068.
13. Balsevich JJ, Cutler AJ, Lamb N, et al. *Plant Physiol.* 1994;106:135.
14. Nyangulu JM, Nelson KM, Rose PA, et al. *Org. Biomol. Chem.* 2006;4:1400.
15. Han X, Jiang L, Che C, et al. *Sci. Rep.* 2017;7:43863.
16. Takeuchi J, Okamoto M, Akiyama T, et al. *Nat. Chem. Biol.* 2014;10:477.
17. G. T. Wang, D. Heiman, G. D. Venburg, J. H. Lustig, M. A. Surpin, R. E. Fritts, F. P. Silverman, D. D. Woolard, WO2016/168535, 2016.
18. G. T. Wang, D. Heiman, G. D. Venburg, E. Nagano, M. A. Surpin, J. H. Lustig, WO2016/007587, 2016.
19. F. P. Silverman, G. Wang, K. A. Falco, D. D. Woolard, D. O. Wilson, D. C. Leep, G. D. Venburg, WO2016/187370, 2016.
20. G. Wang, R. Hopkins, D. C. Leep, D, D. Woolard, G. D. Venburg, WO2016/187370, 2016.
21. Frackenpohl J, Bojack G, Baltz R, et al. *Eur. J. Org. Chem.* 2018:1416.
22. Takeuchi J, Ohnishi T, Okamoto M, Todoroki Y. *Bioorg. Med. Chem. Lett.* 2015;25:3507.
23. Miyakawa T, Tanokura M. *Biophysics.* 2011;7:123.
24. Helander JDM, Vaidya AS, Cutler SR. *Bioorg. Med. Chem.* 2016;24:493.
25. S. R. Cutler, S.-Y. Park, A. Defries, WO2010/093954, 2010.
26. Peterson FC, Burgie ES, Park S-Y, et al. Nature Struct. *Mol. Biol.* 2010;17:1109.
27. J. Frackenpohl, I. Heinemann, T. Müller, P. v. Koskull-Döring, J. Dittgen, D. Schmutzler, C. H. Rosinger, I. Häuser-Hahn, M. J. Hills, WO2011/113861, 2011.
28. S. R. Cutler, M. Okamoto, WO2013/148339, 2013.
29. S. V. Wendeborn, P. J. Jung, M. D. Lachia, R. Dumeunier, S. R. Cutler, WO2014/210555, 2014.
30. J. Frackenpohl, G. Bojack, H. Helmke, S. Lehr, T. Müller, L. Willms, H. Dietrich, D. Schmutzler, R. Baltz, U. Bickers, WO2015/155154, 2015.
31. J. Frackenpohl, G. Bojack, H. Helmke, L. Willms, S. Lehr, T. Müller, J. Dittgen, D. Schmutzler, R. Baltz, U. Bickers, WO2016/128365, 2016.
32. S. R. Cutler, M. D. Lachia, S. V. Wendeborn, C. R. A. Godfrey, D. Sabbadin, WO2018/017490, 2018.
33. Elzinga D, Sternburg E, Sabbadin D, et al. *Biol.* 2019;14:332.
34. Frackenpohl J, Schneider L, Decker LJB, et al. *Bioorg. Med. Chem.* 2019;27:115142.
35. Vaidya AS, Peterson FC, Yarmolinsky D, et al. *Biol.* 2017;12:2842.
36. S. R. Cutler, A. Vaidya, J. Helander, WO2020/006508, 2020.
37. J. Frackenpohl, G. Bojack, H. Helmke, S. Lehr, I. Heinemann, K. Minn, J. Dittgen, D. Schmutzler, U. Bickers, M. J. Hills, F. Roth, F. Poree, EP3210469, 2017.
38. Eto M. *Biosci. Biotech. Biochem.* 1997;61:1.
39. D. Virieux, J.-N. Volle, N. Bakalara, J.-L. Pirat, Synthesis and Biological Applications of Phosphinates and Derivatives. In: Montchamp JL. (eds) Phosphorus Chemistry I. Topics in Current Chemistry, vol 360. Springer, 2014, 39-114.
40. Volle J-N, Guillon R, Bancel F, Bekro Y-A, Pirat J-L, Virieux D. *Adv Heterocycl Chem.* 2016;118:130.
41. Rodriguez JB, Gallo-Rodriguez C. *ChemMedChem.* 2019;14:190.
42. Alexandre F-R, Amador A, Bot S, et al. *J. Med. Chem.* 2011;54:392–395.
43. Reulecke I, Lange G, Albrecht J, Klein R, Rarey M. *ChemMedChem.* 2008;3:885.
44. Li X, Zhang D, Pang H, et al. *Org. Lett.* 2005;7:4919.
45. Campbell DA. *J. Org. Chem.* 1992;57:6331.
46. R. Noe, A. Henne, M. Maase, DE10206117, 2002.
47. H. Helmke, J. Frackenpohl, J. Franke, G. Bojack, J. Dittgen, D. Schmutzler, U. Bickers, F. Poree, F. Roth, J.-P. Vors, WO2017/009321, 2017.
48. Tan C, Liu X, Jia H, et al. *Chem. Eur. J.* 2020;26:881.
49. Raghanvendra AS, Gonugunta VK, Christmann A, Grill E. *Trends Plant Sci.* 2010;15:395.
50. Dupeux F, Antoni R, Betz K, et al. *Plant Physiol.* 2011;156:106.
51. Vagin A, Teplyakov A. *Acta Crystallogr. D.* 2010;66:22.
52. Emsley P, Cowtan K. *Acta Crystallogr. D.* 2004;60:2126.
53. Murshudov GN, Skubak P, Lebedev AA, et al. *Acta Crystallogr. D.* 2011;67:355.